RECEIVED BY TIC AUG 28 1981

LBL-11986

Lawrence Berkeley Laboratory

UNIVERSITY OF CALIFORNIA

ENERGY & ENVIRONMENT DIVISION

MASTER

ENVIRONMENTAL POLLUTANT STUDIES

Chapter from the Energy and Environment Division Annual Report 1980

February 1981

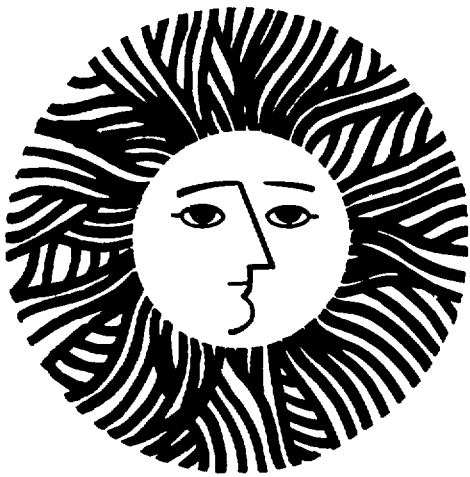

DISTRIBUTION OF THIS DOCUMENT IS UNLIMITED

Prepared for the U.S. Department of Energy under Contract W-7405-ENG-48

ENVIRONMENTAL POLLUTANT STUDIES
FY 1980

DISCLAIMER

Lawrence Berkeley Laboratory
University of California
Berkeley, California 94720

Prepared for the U.S. Department of Energy under Contract W-7405-ENG-48

DISTRIBUTION OF THIS DOCUMENT IS UNLIMITED

CONTENTS

ENVIRONMENTAL POLLUTANT STUDIES PERSONNEL 5-v

ATMOSPHERIC AEROSOL PROJECT

INTRODUCTION
T. Novakov 5-1

Activated Carbon Catalyzed Oxidation of Aqueous S(IV) Species
R. Brodzinsky, S. Chang, S. Markowitz, and T. Novakov 5-1

Oxidation of SO_2 by Wet Soot Particles: Application to Clouds, Fogs, and Plumes
W. Benner, R. Brodzinsky, and T. Novakov 5-5

Aqueous Reactions of Nitrite and Bisulfite
S. Oblath, S. Chang, S. Markowitz, and T. Novakov 5-7

The Importance of Soot Particles and Nitrous Acid in Oxidizing SO_2 in Atmospheric Aqueous Droplets
S. Chang, R. Toossi, and T. Novakov 5-10

Kinetics of the Reaction Between NH_2OH and SO_2 in Aqueous Solutions
S. Gomiscek, R. Clem, T. Novakov, and S. Chang 5-13

The Role of Fly Ash in the Catalytic Oxidation of SO_2
S. Cohen, S. Chang, S. Markowitz, and T. Novakov 5-15

Soot in the Arctic
H. Rosen, T. Novakov, and B. Bodhaine 5-19

An Intercomparison of the Integrating Plate and the Laser Transmission Methods for Determination of Aerosol Absorption Coefficients
M. Sadler, R. Charlson, H. Rosen, and T. Novakov 5-23

Determination of Black Carbon by Thermal Analysis
L. Gundel, R. Dod, and T. Novakov 5-26

A Model for the Progressive Combustion Analysis of Carbonaceous Aerosol Particles
A. Hansen and T. Novakov 5-30

Relation Between Concentrations of Polynuclear Aromatic Hydrocarbons and Black Carbon
L. Gundel, H. Rosen, and T. Novakov 5-32

Determination of Carbon in Atmospheric Aerosols by Deuteron-Induced Nuclear Reactions
M. Clemenson, T. Novakov, and S. Markowitz 5-35

Determination of Low-Z Elements Simultaneously by ^{3}He-Induced Nuclear Reactions
M. McKinney and S. Markowitz 5-38

MEMBRANE BIOENERGETICS RESEARCH

Membrane Oxidative Damage
L. Packer, A. Quintanilha, R. Mehlhorn, O. Augusto, J. Maguire, and K. Davies 5-40

LAKE ECOTOXICOLOGY RESEARCH

INTRODUCTION
J. Harte 5-43

Assessment of Optimum Microcosm Design for Pollution Impact Studies
J. Harte, D. Levy, J. Rees, and E. Saegebarth 5-43

Acid Precipitation Damage to Aquatic Ecosystems
J. Harte, K. Tonnessen, R. Schneider, G. Lockett, and J. Oldfather 5-47

ENVIRONMENTAL POLLUTANT STUDIES PERSONNEL

FY 1980

Atmospheric Aerosol Research Group

Tihomir Novakov, Group Leader
William Benner
Richard Brodzinsky
Shih-Ger Chang
Mark Clemenson
Sidney Cohen
Ray Dod
Sergei Gomiscek*
Lara Gundel
Anthony Hansen
Samuel Markowitz
Michael McKinney
Steven Oblath
Hal Rosen
Richard Schmidt
Reza Toossi
Linda Wroth

Lake Ecotoxicology Group

John Harte, Group Leader
Michael Dudzik
Don Levy
Gregory Lockett
Joan Oldfather
John Rees
Ellen Saegebarth
Richard Schneider
Kathy Tonnessen

Membrane Bioenergetics Group

Lester Packer, Group Leader
Anne Lewis
John Maguire
Rolf Mehlhorn
Alex Quintanilha
Brenda Soares

*On leave from the University of Ljubljana, Yugoslavia.

ATMOSPHERIC AEROSOL PROJECT

INTRODUCTION

T. Novakov

The principal research interest of the Atmospheric Aerosol Research group is in determining the role of primary particles in atmospheric chemistry and physics. Specifically, we are interested in heterogeneous atmospheric chemical reactions that involve primary particles, such as soot and fly ash, and gaseous species, and in the effects of primary particles on visibility and climate. This research entails laboratory studies complemented by selective field sampling and experiments. All our studies rely on analytical chemistry and other measurement sciences. We are therefore actively developing methods for chemical characterization of aerosol particles and for determining their optical properties.

In the field of atmospheric chemistry, we have primarily focused on the formation of sulfates by aqueous reactions catalyzed by solid particles and dissolved metal ions. In addition, the role of the oxides of nitrogen in SO_2 oxidation was also studied.

During recent years, we have definitely established that black graphitic carbon is a major constituent of the carbonaceous fraction of urban aerosol particles. During the past year, measurements were extended to the Arctic region, where a substantial concentration of these particles was determined. The impacts of these highly absorbing species on climate have not yet been assessed, but preliminary studies indicate that they could be very important, especially over regions with a high surface albedo, such as the polar ice caps.

In methods development, we have been working on determining aerosol absorption coefficients, developing thermal analysis methods (combined with optical measurements and solvent extraction procedures) to study carbonaceous and nitrogenous species, and further developing deuteron and ^{3}He-induced activation analysis for determination of low-Z elements in aerosol particles.

ACTIVATED CARBON CATALYZED OXIDATION OF AQUEOUS S(IV) SPECIES*

R. Brodzinsky, S. Chang, S. Markowitz, and T. Novakov

INTRODUCTION

The formation of acid rains is a source of major interest and concern. Acid rain is caused by nitric and sulfuric acids that are formed by the oxidation of nitrogen oxides (NO_x) and sulfur dioxide (SO_2). The precipitation's increased acidity as much as pH ~3 in parts of New England and Europe instead of the "normal" of pH ~5.6) has had many deleterious effects. Many lakes have become too acidic to sustain aquatic life; most fish cannot live in water with a pH <4.5.[1] The acidity also affects plant life, both by attacking the vegetation's leaves and branches and by leaching nutrients from the soil. Acidity also has its effects on buildings and statues. Many older structures, especially those constructed of sandstone or marble, are literally dissolving.

*This work was supported by the Assistant Secretary for Environment, Office of Health and Environmental Research, Division of Biomedical and Environmental Research of the U.S. Department of Energy under Contract No. W-7405-ENG-48 and by the National Science Foundation under Contract No. ATM 80-13707.

Many mechanisms are known for the oxidation of SO_2.[2] We have been studying the catalytic effects of carbonaceous soot particles and activated carbons on this reaction.[3] Carbonaceous particles in aqueous suspension were found to be efficient catalysts for the oxidation of aqueous sulfur (IV) [S(IV)] species.

Those studies' kinetic results showed that the reaction followed a Langmuir adsorption isotherm for its rate dependence on dissolved O_2 and the product of two adsorption isotherms for S(IV). The rate of reaction is linearly dependent on the concentration of carbon particles in the solution. (Note: Hydrated sulfur dioxide ($SO_2 \cdot H_2O$) is also known as "sulfurous acid" (H_2SO_3), but this molecule has never been observed. Within this work the symbol S(IV) and the formula H_2SO_3 are used to signify all the S(IV)-containing species in solution ($SO_2 \cdot H_2O$, HSO_3^-, and SO_3^{2-}). The symbol C_x signifies the carbonaceous particle surface, while the term "carbon" refers to the particles of activated carbon or soot and not the element C.)

We propose a possible four-step reaction mechanism which consists of the adsorption of a dissolved O_2 molecule onto the carbon surface,

followed by the adsorption of 2 S(IV) molecules or ions. These are oxidized on the surface to sulfate, which desorbs from the surface, regenerating the catalytically active site.

We have extended this research to other activated carbons and to soot collected in a highway tunnel.

ACCOMPLISHMENTS DURING FY 1980

The following experimental methods were used. A known amount of S(IV) was added to the basic reaction system, consisting of a flask in which carbonaceous particles were suspended in deionized water. Three different commercially available activated carbons were used: Nuchar C-190 and Nuchar S-N, manufactured by the West Virginia Pulp and Paper Co. (Wesvaco), and EM Reagents, Aktivkohle, manufactured by E. Merck.

The Aktivkohle is a 30-50 mesh activated carbon for use in gas chromatography. It was ground in an agate ball mill for 15 h to produce a powder of ~200 mesh. The two Nuchars are decolorizing carbons of 200-400 mesh. The manufacture of C-190 was discontinued in 1978. The activated carbons were washed three times with boiling water to remove water soluble sulfates and nitrates that were adsorbed on the surface, and then the carbons were dried. Elemental analysis and physical properties of the activated carbons are shown in Table 1.

Automotive soot was collected in the ventilation duct above the Caldecott Tunnel, a 1.5-mile highway tunnel on California Route 24 beneath the Berkeley hills between Oakland and Orinda. A ventilation tunnel above the roadway is coated with automotive soot. This soot was scraped from the walls with a plastic scraper into a large plastic bucket. It was then washed three times with boiling water and dried. The water wash removed the

Table 1. Elemental analysis of carbons (w%).

Element	C-190	SN	Aktivkohle	Tunnel	Method
C	74.7	77.7	88.1	14.2	Combustion
H	0.9	1.56	1.60	1.75	Combustion
N	0.1	0.23	1.17	0.30	Combustion
Ca	0.221	b.d.	0.025	1.98	XRF
S	0.116	0.07	0.39	1.15	XRF
Si	>0.111	b.d.	b.d.	>10.1	XRF
Fe	0.117	0.011	0.018	2.83	XRF
K	0.091	b.d.	b.d.	b.d.	XRF
Al	>0.055	b.d.	b.d.	>4.05	XRF
Ti	0.016	0.0017	b.d.	0.122	XRF
Mn	0.013	0.0012	b.d.	0.022	XRF
Cr	0.002	0.0011	b.d.	0.014	XRF
Cu	0.002	0.0007	b.d.	0.018	XRF
Zn	0.002	0.0006	0.117	0.122	XRF
Sr	0.002	b.d.	b.d.	0.086	XRF
Ni	0.001	b.d.	0.002	0.108	XRF
Cl	0.001	b.d.	0.001	0.101	XRF
As	0.0004	b.d.	b.d.	b.d.	XRF
Br	0.0004	b.d.	0.001	0.007	XRF
Rb	0.0004	b.d.	b.d.	b.d.	XRF
Zr	0.0004	b.d.	b.d.	b.d.	XRF
Pb	0.0004	b.d.	0.007	5.06	XRF
Ga	0.0001	b.d.	b.d.	b.d.	XRF
Ba	b.d.	b.d.	b.d.	0.158	XRF
O	23.6	20.4	8.57	<57.8	Difference
Surface area (m^2/g)	550	1150	1130	6	
Activation temperature (°C)	650	650	300		
pH (1g/ℓ)	5.4	7.2	6.2	5.0	
Made from	coal	coal	peat		

b.d. = below detection limits.
XRF = X-ray fluorescence technique.

water soluble organics, as well as the inorganics, which had adsorbed onto the soot surface. The composition and physical properties of the tunnel soot are shown in Table 1.

The dependence of the reaction rate on S(IV) concentration for the four different carbons is shown in Figure 1. Oxygen- and temperature-dependence data for the activated carbons are shown in Figures 2 and 3 respectively. Table 2 summarizes the coefficients for the experimentally seen rate law for the activated carbons. Oxygen and temperature studies were not performed on the tunnel soot. Within the experimental rate law for the tunnel soot,

$$k = Ae^{-Ea/RT} \frac{\gamma[O_2]}{1+\gamma[O_2]} = 1.97 \times 10^{-7} \text{ mol/g·s}$$

$\alpha = 6.36 \times 10^{6}$ l^2/mol^2

$\beta = 9.93 \times 10^{2}$ l/mol

Ea = activation energy

R = gas constant

T = temperature

γ = adsorption constant

Our proposed mechanism for this reaction is:

$$C_x + O_2(aq) \underset{k_{-1}}{\overset{k_1}{\rightleftarrows}} C_x{\cdot}O_2 \qquad (1)$$

$$C_x{\cdot}O_2 + S(IV) \underset{k_{-2}}{\overset{k_2}{\rightleftarrows}} C_x{\cdot}O_2{\cdot}S(IV) \qquad (2)$$

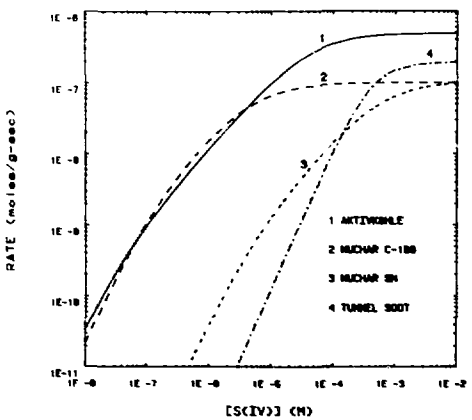

Fig. 1. Normalized rate of reaction versus total S(IV) concentration for various activated carbons and tunnel soot. (XBL 8010-12601)

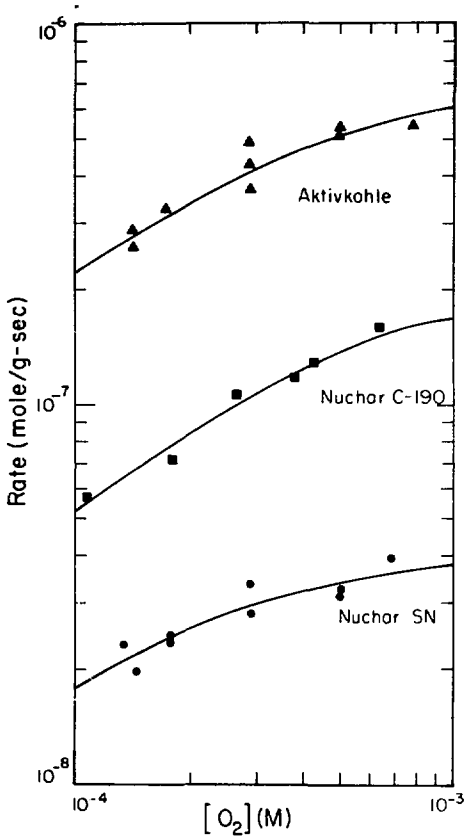

Fig. 2. Normalized rate of reaction versus dissolved oxygen concentration. $[S(IV)] = 5 \times 10^{-4}$ M. (XBL 8010-2279)

$$C_x{\cdot}O_2{\cdot}S(IV) + S(IV) \underset{k_{-3}}{\overset{k_3}{\rightleftarrows}} C_x{\cdot}O_2{\cdot}S^2(IV) \qquad (3)$$

$$C_x{\cdot}O_2{\cdot}S^2(IV) \overset{k_4}{\rightarrow} C_x + 2S(VI) \qquad (4)$$

with

$$\frac{d[S(VI)]}{dt} = 2k_4[C_x]\left(\frac{K_1[O_2]}{1 + K_1[O_2]}\right)\left(\frac{K_2[S(IV)]}{1 + K_2[S(IV)]}\right)\left(\frac{K_3[S(IV)]}{1 + K_3[S(IV)]}\right)$$

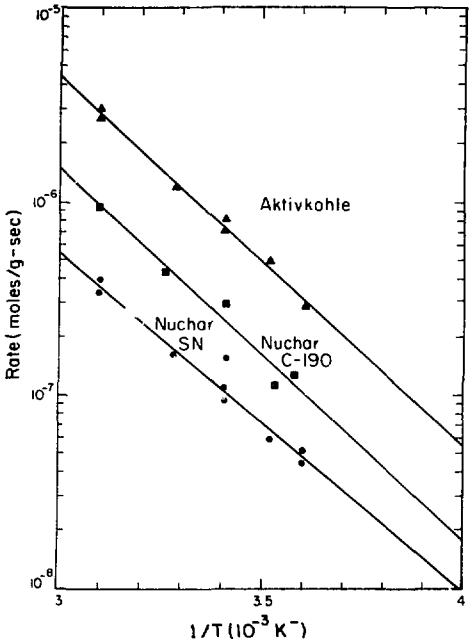

Fig. 3. Normalized rate of reaction versus 1/T (Arrhenius plot). (XBL 8010-2280)

where $K_1 = k_1/k_{-1}$, $K_2 = k_2/k_{-2}$ and $K_3 = k_3/k_{-3}$. Multiplication of the S(IV) terms yields the experimentally seen expression where $K_2K_3 = \alpha$, $K_2 + K_3 = \beta$ and $K_1 = \gamma$.

PLANNED ACTIVITIES FOR FY 1981

Work is currently in progress to determine the catalytic activity of true ambient aerosols. The results of these experiments will be of immeasurable help in determining the contribution of the carbon-catalyzed oxidation of SO_2 to the formation of atmospheric sulfates and acid rain.

REFERENCES

1. S. West, "Acid from Heaven," Science News, vol. 117, 1980, p. 76.
2. D. Möller, "Kinetic Model of Atmospheric SO_2 Oxidation," Atmospheric Environment, vol. 14, 1980. p. 1067.
3. R. Brodzinsky, S. G. Chang, S. S. Markowitz, and T. Novakov, "Kinetics and Mechanism for the Catalytic Oxidation of Sulfur Dioxide on Activated Carbon in Aqueous Suspension," Journal of Physical Chemistry, vol. 84, 1980, p. 3354.

Table 2. Summary of kinetic data for S(IV) oxidation on activated carbons.*

	Activated-Carbons		
	C-190	SN	Aktivkohle
A (mole/g-sec)	0.874	0.158	2.47
E_a (kcal/mole)	8.8	8.1	8.8
γ (ℓ/mole)	2.10×10^3	7.43×10^3	4.37×10^3
α (ℓ^2/mole^2)	2.40×10^{12}	4.92×10^8	9.52×10^{11}
β (ℓ/mole)	1.22×10^7	2.96×10^5	3.74×10^7
r^2 (oxygen)	0.978	0.851	0.925
r^2 (Arrhenius)	0.961	0.952	0.993

*

$$\frac{d[SO_4^{2-}]}{dt} = Ae^{-E_a/RT}[C_x]\left\{\frac{[O_2]}{1+[O_2]}\right\}\left\{\frac{\alpha[S(IV)]^2}{1+\beta[S(IV)]+\alpha[S(IV)]^2}\right\}$$

$\sigma_A^2 = \pm 10\%$

$\sigma_E^2 = \pm 5\%$

$\sigma_\alpha^2 = \sigma_\beta^2 = \sigma_\gamma^2 = \pm 3\%$

OXIDATION OF SO_2 BY WET SOOT PARTICLES: APPLICATION TO CLOUDS, FOGS, AND PLUMES*

W. Benner, R. Brodzinsky, and T. Novakov

INTRODUCTION

Concentrations of $SO_4^=$ and H^+ ions in acid rain are strongly correlated, and therefore the formation of atmospheric $SO_4^=$ is thought to be related to the formation of acid rain.[1] We are constantly revising our understanding of the chemical and physical processes that introduce sulfate into the atmosphere. Our recent studies have been directed towards sulfate formation pathways which involve liquid water. Work in our laboratory[2] has shown that aqueous suspensions of diesel, propane, and natural gas soot particles and several activated carbons oxidize SO_2 to SO_4. The work reported here is an extension of these earlier findings and focuses on the oxidation of SO_2 by dispersed water droplets that contain soot particles.

In laboratory studies, the exposure of dispersed wet soot particles to SO_2 simulates reactions which could occur in clouds, fogs, and plumes. Such dispersed droplet studies would also supply information that could be introduced into computer models to evaluate the relative importance of the soot-fog-SO_2 mechanisms for sulfate formation in the atmosphere. To meet our experimental objectives, we constructed a fog chamber in which stable fogs could be exposed to pollutant gases. The fog chamber work presented in this paper is not intended as a rigorous kinetic study; these experiments were conducted to show that SO_2 can be oxidized in droplets that contain soot particles.

ACCOMPLISHMENTS DURING FY 1980

Particles of Nuchar-SN, pre-extracted to remove SO_4, were resuspended by nebulization, and the resultant mist was passed over heated water and subsequently cooled to cause the nebulized particles to grow into larger droplets (Fig. 1). These droplets were exposed to SO_2 and introduced into the bottom of the fog chamber. The fog droplets were forced upwards through the chamber at a velocity which permitted an approximately 30-min reaction time between droplets and SO_2. A prefired quartz fiber filter and a Fluoropore (0.5-μm pore) filter were used simultaneously to collect samples from the top of the chamber. The filter holders and tubing leading to the filters were heated to decrease the relative humidity of the air stream to at least 30%, and reactions involving liquid water were thereby prevented. After collection of the sample, the Fluoropore filter was extracted in water and analyzed for SO_4 using ion chromatography. A portion of the quartz filter was analyzed for total carbon by combustion analysis.

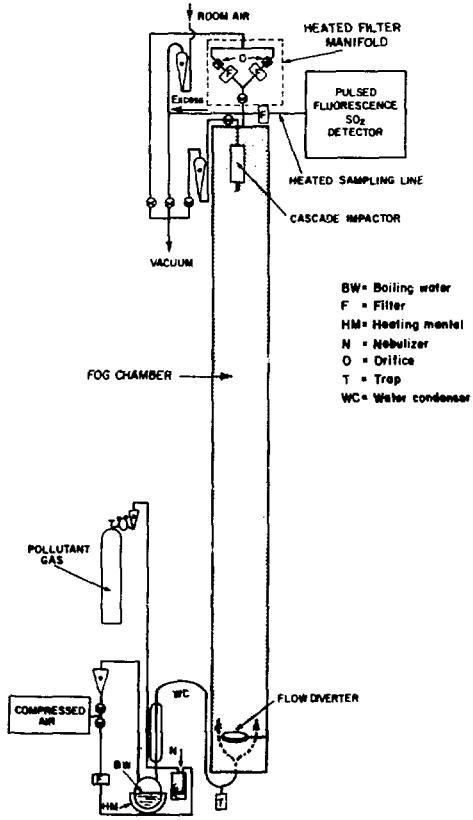

Fig. 1. Laboratory fog chamber and associated equipment. (XBL 804-4124)

When pure water droplets were exposed to SO_2 in the fog chamber, the rate of SO_4 formation ($\mu g\ SO_4/m^3 \cdot h$) equals 4.06 (ppm SO_2)$^{.0007}$ (Fig. 2). If the droplets contained Nuchar-SN particles, the rate of SO_4 formation was found to be significantly faster than for pure water droplets. For example, wet soot particles exposed to 0.007 ppm SO_2 produced SO_4 faster than pure water droplets exposed to 222 ppm SO_2. The data for SO_4 formation by wet soot particles is plotted with open circles in Figure 2. When the soot-droplet data in Figure 2

*This work was supported by the Department of Energy under Contract No. W-7405-ENG-48 through the Environmental Protection Agency under Contract No. 79-D-X-0533.

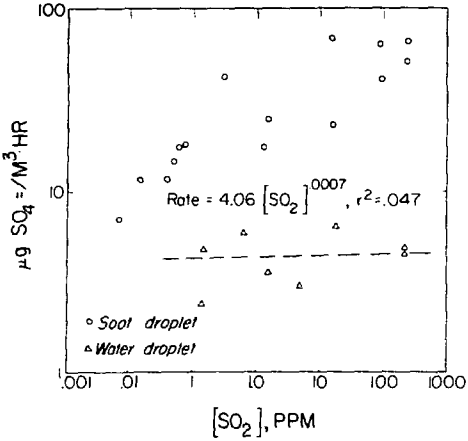

Fig. 2. Production of SO_4 in fog droplets versus SO_2. (XBL 809-1861)

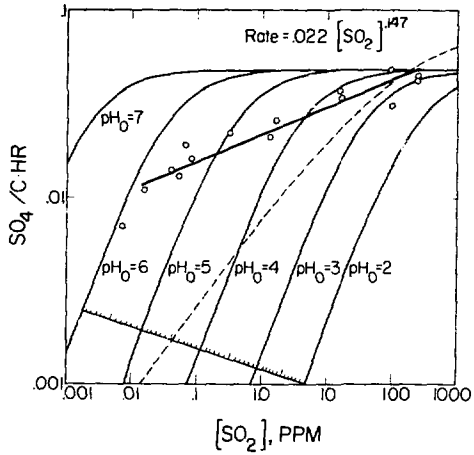

Fig. 3. The normalized rate of SO_4 formation in wet soot droplets vs. SO_2. The open circles and the solid line drawn through the circles were obtained from fog chamber data. The family of curves labelled $pH_0 = 2$ through $pH_0 = 7$ was calculated from Equation 1. pH_0 is the pH of droplets in equilibrium with SO_2 and CO_2 before the start of the reaction. The dashed line shows the rate for SO_4 formation (Eq. 1) for wet soot droplets whose pH before exposure to SO_2 and 320 ppm CO_2 is determined by SO_2-CO_2-H_2O equilibria. The dashed line is juxtaposed on pH coordinates created by the family of curves labelled $pH_0 = 2$ through $pH_0 = 7$. (XBL 809-1860)

are normalized to [C], the carbon-normalized rate of SO_4 formation can be plotted as shown in Figure 3 (open circles). The equation which best fits the carbon-normalized soot droplet data is $SO_4^{2-}/C \cdot h = 0.222(SO_2)^{.147}$.

In Figure 3, a family of curves is presented which shows the rate of SO_4 formation, normalized to C, as a function of $[SO_2]$ for various initial $[H^+]$'s. This family of curves was calculated from the following rate expression:[3]

$$\frac{d[S(IV)]}{dt} = k(C) \frac{[S(IV)]^2}{1 + \beta[S(IV)] + \alpha[S(IV)]^2} \qquad (1)$$

where [C] = soot concentration in droplet, (g/ℓ)

$[S(IV)] = [SO_2 \cdot H_2O] + [HSO_3^-] + [SO_3^=]$

$\alpha = 4.915 \times 10^8\ l^2/mol^2$

$\beta = 2.956 \times 10^5\ l/mol$

$k = 1.336 \times 10^{-7}\ mol/g \cdot s$

The family of curves in Figure 3 indicates a pH effect on sulfate formation, but pH only becomes a factor when soot suspensions are exposed to SO_2. The pH effect is related to the absorption of SO_2 by the droplet. For example, two droplets, one of which has an initial pH of 3 and the other a pH of 5, are equilibrated with 1 ppm SO_2. The droplet with the lower initial pH will have a lower equilibrium [S(IV)] and the oxidation rate will be similarly slower. The family of curves was calculated assuming that the droplet had a specified initial pH and equilibrated with SO_2 and 320 ppm CO_2 to produce a certain equilibrium [S(IV)] before the oxidation started. The resultant [S(IV)] was then used to calculate the reaction rate using Equation 1.

The dashed line in Figure 3 shows the S(IV) oxidation rate expected for wet soot particles in equilibrium with SO_2. This curve was calculated assuming that the soot droplet initially had a pH of 7 and was then equilibrated with SO_2 and 320 ppm CO_2 to produce a certain equilibrium [S(IV)] and equilibrium pH before oxidation started. The resulting [S(IV)] was used to calculate the reaction rate using Equation 1. It was also assumed in the calculation that the soot possessed no pH-altering species.

The difference between the fog chamber data and the dashed line in Figure 3 is due to the alkaline nature of Nuchar-SN. The release of alkaline species into the droplet from the Nuchar SN neutralized some of the absorbed $SO_2 \cdot H_2O$ and/or HSO_3^-, and thus the equilibrium [S(IV)] was larger than that predicted by Henry's Law for pure water and SO_2. This neutralization increased the oxidation rate because it brought more $SO_2 \cdot H_2O$ and HSO_3 into the droplet. The magnitude of the difference between the fog chamber data line and the dashed line depends on the $[SO_2]$. At low $[SO_2]$, the alkaline species on the soot particles attract into solution more $SO_2 \cdot H_2O$ or HSO_3^- than would be expected for pure water, and thus these alkaline species strongly influence the resultant [S(IV)]. At high $[SO_2]$, the dissolved SO_2 becomes the dominant factor

for controlling the resultant [S(IV)]. Therefore, at high [SO_2], the fog chamber data line and the dashed line in Figure 3 coincide.

Data presented here show that dispersed wet soot particles (Nuchar-SN being a type of soot) can oxidize SO_2 to sulfate. This indicates that the SO_2 oxidation mechanism (Eq. 1) can be applied to the troposphere. These data also confirm predictions made by others in our laboratory[4] which indicated that the oxidation of SO_2 by wet soot particles is an important tropospheric source of particulate sulfate.

PLANNED ACTIVITIES FOR FY 1981

The fog chamber experiments will be continued to include other types of wet soot particles.

REFERENCES

1. G. E. Likens, R. F. Wright, J. N. Galloway, and T. J. Butler, "Acid Rain," Scientific American, vol. 241, 1979, p. 43.

2. R. Brodzinsky, S. G. Chang, S. S. Markowitz, and T. Novakov, "Kinetics and Mechanism for the Catalytic Oxidation of Sulfur Dioxide on Carbon in Aqueous Suspensions," Journal of Physical Chemistry, vol. 84, 1980, p. 3354.

3. R. Brodzinsky, Catalytic Oxidation of S(IV) on Activated Carbon in Aqueous Suspension: Kinetics and Mechanism, Ph.D. dissertation, University of California, Berkeley, 1981.

4. R. Toossi, T. Novakov, and S. G. Chang, "Relative Importance of Various Sulfate Production Mechanisms in Aqueous Droplets," in Atmospheric Aerosol Research Annual Report 1977-78, Lawrence Berkeley Laboratory report LBL-8696, 1978.

AQUEOUS REACTIONS OF NITRITE AND BISULFITE*

S. Oblath, S. Chang, S. Markowitz, and T. Novakov

INTRODUCTION

In studies of particulate sulfate formation, it is important to know what role the oxides of nitrogen (NO_x) will play, as they are both abundant pollutants. This question may be of even greater importance with respect to aerosol droplets, as both SO_2 and NO_x are soluble gases. Homogeneous reactions involving the two gases have been studied for a number of years.[1] More recently studies have been undertaken to determine the effect of NO_x on heterogeneous sulfate formation.[2,3]

Several years ago we began a study to investigate the reactions of nitrite (NO_2^-) and bisulfite (HSO_3^-) as a first step toward understanding the $NO_x/SO_2/H_2O$ system. Nitrite is known to react with bisulfite over a wide range of conditions. Previous work by other scientists[4-6] reported conflicting results and left several questions unanswered. The experiments which we performed have clarified many of these questions and are reported in a recent publication.[7]

All the known aqueous reactions of nitrite with bisulfite begin with the formation of hydroxylamine disulfonate (HADS). The results of our previous work may be summarized by the following rate expression:

$$\text{Rate} = K_A[H^+][NO_2^-][HSO_3^-] + k_B[NO_2^-][HSO_3^-]^2 \quad .$$

This rate law is valid over the pH range of 4.5 to 7. Work has been progressing during the past year to answer several remaining questions pertaining to the formation of HADS: (1) Is a process independent of bisulfite concentration really present, as noted in the literature; (2) What role will carbon particles have in this reaction; and (3) What effect will extremely low reactant concentrations (or high acidity) have on the products or rate of the nitrite-bisulfite reaction.

ACCOMPLISHMENTS DURING FY 1980

Bisulfite Independent Pathway

A HADS formation pathway that is independent of bisulfite ion concentration is of importance to atmospheric chemists as the rate is not affected when the SO_2 concentration is lowered to ambient levels. Previous researchers had identified a process of this type.[4,6] We have carried out experiments to determine the presence or absence of this pathway by addition of $NaNO_2$ to buffered solutions of bisulfite ion under pseudo-first-order conditions. Nitrite concentrations (initially 3.5

*This work was supported by the Assistant Secretary for Environment, Office of Health and Environmental Research, Division of Biomedical and Environmental Research Division of the U.S. Department of Energy under Contract No. W-7405-ENG-48, and the Morgantown Energy Research Center under Contract No. AA 050515.

to 10 mM) were monitored by visible spectrophotometry as in our previous work. Bisulfite ion concentration was between 5 and 40 mM. The pH was maintained by using oxalate, tartrate, or phthalate buffers of an ionic strength of 0.2 M.

Results of these experiments are shown in Figure 1. The zero intercepts show that there is no process occurring which is independent of bisulfite concentration. The buffers that were used overlap in their pH ranges, and tests in different buffers show no evidence of inhibitory or catalytic effect. Tests carried out at differing buffer concentrations (ionic strength maintained at 0.2 M) again show no inhibiting effect of the buffer. Previous work was carried out in acetate buffers, a medium believed to stabilize NO^+ formation. (NO^+ is the predicted intermediate for a bisulfite independent pathway.) Although NO^+ may be formed, the rate in the absence of acetate is too slow to be important at pH's accessible to ambient aerosol droplets.

Effect of Carbon

Since aerosol droplets are often formed around carbonaceous particles, it is important to understand the effects of carbon on this set of reactions. A finely ground activated carbon (Nuchar SN) was used at a concentration of approximately 0.1% by weight. This is about what would be expected in a wet aerosol. Reaction conditions were the same as in the previous study, except that aliquots of the solution were filtered before the nitrite was measured. Blank runs (no carbon present) showed that filtering had no effect on the results. A sulfite-bisulfite buffer was used, which insures pseudo-first-order conditions. The results with and without carbon agree well, which indicates Nuchar SN has no effect on the reaction. After long reaction times, the runs with carbon proceed more slowly. This is consistent with the oxidation of HSO_3^- on the Nuchar[8] and the breakdown of pseudo-first-order conditions.

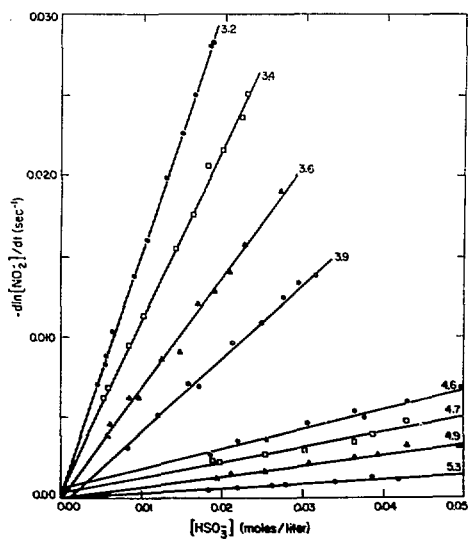

Fig. 1. Experimental rates as a function of bisulfite ion concentrations. Numbers indicate the pH for each set of reactions. (XBL 8011-2377)

Effect of Low Concentration or High Acidity on the Reaction

Prior to determining the rate of HADS formation at lower pH's, we determined the stoichiometry by determining the changes in concentrations of bisulfite (by iodometry) and nitrite (by spectrophotometry). The initial HSO_3^- concentration was always greater than twice that of NO_2^- to insure that HADS could form. The pH was measured at the start of each experiment. The results are shown in Figures 2 and 3. As one goes to pH less than 3, the stoichiometric ratio ($\Delta S/\Delta N$) ratio begins to decrease from 2 to 1, and some other product is being formed. The same trend is seen if one maintains a constant pH and lowers the bisulfite concentration. This indicates that some intermediate is reacting to form another product, most likely N_2O.

To test this hypothesis, several trials were carried out in a flask sealed with a rubber septum. The gas above the solution was then analyzed using gas chromatography with a Porapak Q column and a thermal conductivity detector. Typical results (Fig. 4) indicate that N_2O is the product when $\Delta S/\Delta N = <2$.

In going to very low (micromolar) concentrations, the competition for the intermediate becomes very important because the pH of the droplet will remain roughly constant while the bisulfite ion concentration drops. The studies at high acidity allow us to estimate the relative magnitude of the rate constants and thus determine the branching ratio under different conditions. To do this, we assume a system as follows:

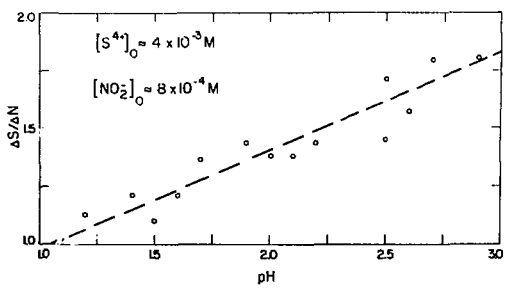

Fig. 2. Stoichiometric ratio at various pH's. (XBL 8011-2381)

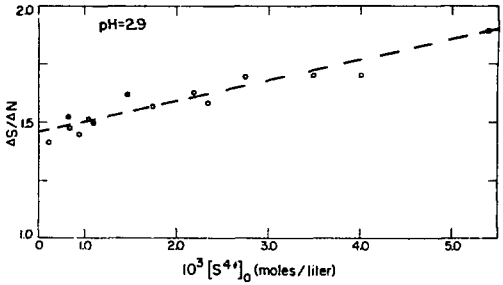

Fig. 3. Stoichiometric ratio at various bisulfite ion concentrations at a fixed acidity.
(XBL 8011-2380)

$$\text{HONO} + HSO_3^- \xrightarrow{HSO_3^-} \text{intermediate} \xrightarrow[1]{} \text{HADS} \quad .$$

$$\text{intermediate} \xrightarrow{2\ H^+} \text{NOH (or } N_2O)$$

The value of $\Delta S/\Delta N$ is related to the amount of products formed and is therefore related to the ratio $k_1[HSO_3^-]/k_2[H^+]$. By taking the data presented in Figures 2 and 3, we have determined the ratio k_1/k_2 to be 1.7 ± 0.5. Therefore, whenever the H^+ ion concentration is much greater than that of bisulfite ion, the major product will be N_2O, with SO_4 being the fate of the SO_2. Under typical ambient conditions, N_2O will most likely be the N-containing product which is formed. The rate limiting step should remain the same as that for HADS formation.

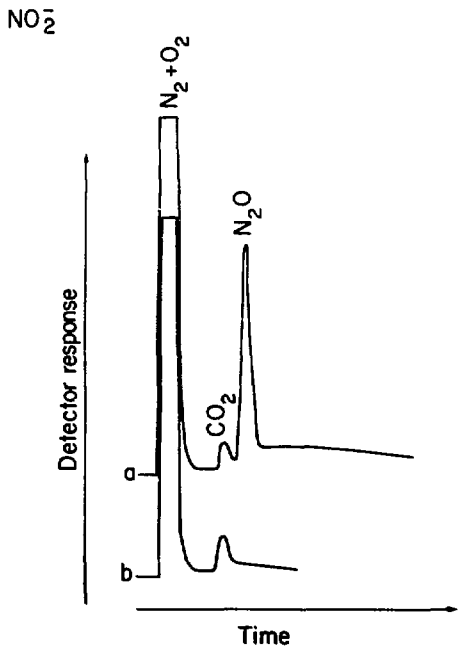

Fig. 4. Chromatogram of gaseous products. Curve a for $\Delta S/\Delta N = 1.4$; curve b for $\Delta S/\Delta N = 2$.
(XBL 8011-2382)

Conclusions

The work which has been described here will enable the modeling of one set of reactions of NO_x and SO_2 under a wide range of conditions. The fates of both the N and S have been determined. The kinetics of this system indicates a strong dependence on reactant concentrations. The increase in rate with increase in acidity will counter the effect of decreasing solubility of the gases with increasing acidity.

PLANNED ACTIVITIES FOR FY 1981

Future work will include an investigation of reactions of HADS with NO_2^- and hydroxylamine monosulfonate with NO_2^-. This will allow us to determine the fate of N and S over a more complete range of conditions than is currently possible.

REFERENCES

1. J. G. Calvert, F. Su, J. W. Bottenhiem, and O. P. Strausz, "Mechanism of the Homogeneous Oxidation of Sulfur Dioxide the Troposphere," Atmospheric Environment, vol. 12, 1978, p. 197.

2. L. G. Britton and A. G. Clarke, "Heterogeneous Reactions of Sulphur Dioxide and SO_2/NO_2 Mixtures with a Carbon Soot Aerosol," Atmospheric Environment, vol. 14, 1980, p. 829.

3. W. R. Cofer, III, D. R. Schryer, and R. S. Rogowski, "The Enhanced Oxidation of SO_2 by NO_2 on Carbon Particulates," Atmospheric Environment, vol. 14, 1980, p. 571.

4. V. F. Seel and E. Degener, "Kinetik und Chemismus der Raschigschen Hydroxylamin-Synthese," Zeitschrift für Anorganische und Allegemeine Chemie, vol. 284, 1956, p. 100.

5. V. F. Seel and H. Knorre, "Die Umsetzung von Nitrit mit Hydrogensulfit in Hydrogensulfit-Sulfit-Pufferlösungen," Zeitschrift für Anorganische und Allegemeine Chemie, vol. 313, 1961, p. 70.

6. S. Yamamoto and T. Kaneda, "Kinetics of Formation of Hydroxylaminedisulfonate and Nitrilosulfonate by Raschig's Hydroxylamine Process," Nippon Kagaku Zasshi, vol. 80, 1959, p. 1098.

7. S. B. Oblath, S. S. Markowitz, T. Novakov, and S. G. Chang, "Kinetics of the Formation of Hydroxylamine Disulfonate by Reaction of Nitrite with Sulfites," Journal of Physical Chemistry, vol. 85, 1981, p. 1017.

8. R. Brodzinsky, S. G. Chang, S. S. Markowitz, and T. Novakov, "Kinetics and Mechanism for the Catalytic Oxidation of Sulfur Dioxide on Carbon in Aqueous Solutions," Journal of Physical Chemistry, vol. 84, 1980, p. 3354.

THE IMPORTANCE OF SOOT PARTICLES AND NITROUS ACID OXIDIZING SO_2 IN ATMOSPHERIC AQUEOUS DROPLETS*

S. Chang, R. Toossi, and T. Novakov

INTRODUCTION

Sulfuric and nitric acids make a major contribution to the acidity of rain water. These acids are produced primarily from the oxidation of SO_2 and NO_x by homogeneous and/or heterogeneous processes in the atmosphere. The dominant mechanisms responsible for this transformation have not yet been established. In our laboratory we found two previously unrecognized reaction pathways which involve water droplets and could be important processes in the genesis of acid rain and sulfate aerosols: (1) oxidation of SO_2 in water droplets containing soot particles[1,2] and (2) oxidation of SO_2 by HNO_2 in water droplets.[3] Here we discuss the impact of these two systems on atmospheric sulfate aerosol formation.

ACCOMPLISHMENTS DURING FY 1980

For the oxidation of SO_2 in water droplets containing soot particles, the reaction rate law can be expressed by the following equation:

$$\frac{d[S(VI)]}{dt} = k[C_x]\, O_2^{0.69} f[S(IV)], \qquad (1)$$

$$\text{where } f[S(IV)] = \left\{\frac{\alpha\,[S(IV)]^2}{1 + \beta[S(IV)] + \gamma[S(IV)]^2}\right\},$$

$[C_x]$ = grams of carbon particles/l,

$[O_2]$ = moles of dissolved oxygen/l, and

$[S(IV)]$ = total moles of S(IV)/l.

The dependence of the rate of formation of sulfate on the partial pressure of SO_2 (P_{SO_2}) in the atmosphere can be obtained from Equation 1.

Because the effect of P_{SO_2} on the rate is contained in f[S(IV)], we illustrate the relationship of f[S(IV)] with P_{SO_2} and pH of the aqueous droplets as shown in Figures 1 and 2. The f[S(IV)], or the rate of production of sulfate (because the rate is linearly proportional to f[S(IV)]), decreases as the pH decreases at a given P_{SO_2}. The magnitude of f[S(IV)]'s changing per unit pH change is much larger at a lower P_{SO_2}. Also f[S(IV)] (or the rate) depends only slightly on P_{SO_2} under most atmospheric conditions when P_{SO_2} is between 1 and 10 ppb and the pH ranges between 5 and 6. The f[S(IV)] increases only 10% and 100% respectively at pH of 6 and 5 when P_{SO_2} increases from 1 to 10 ppb. However, f[S(IV)] depends strongly on P_{SO_2} when the pH is low.

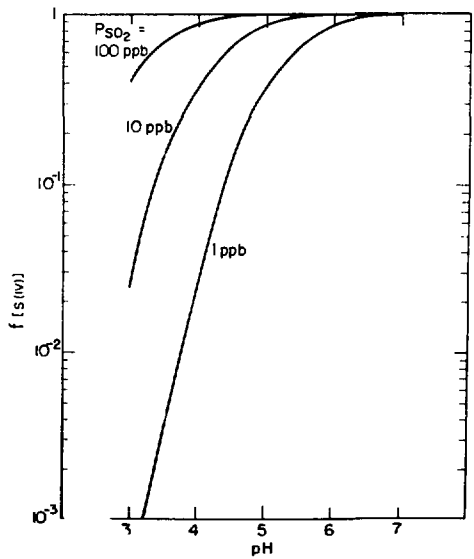

Fig. 1. The effect of the pH of aqueous droplets on f[S(IV)] is a function of S(IV) on which the aqueous oxidation rate of sulfites on soot particles depends. (XBL 808-5732)

*This work was supported by the Assistant Secretary for Environment, Office of Health and Environmental Research, Division of Biomedical and Environmental Research of the U.S. Department of Energy under Contract No. W-7405-ENG-48.

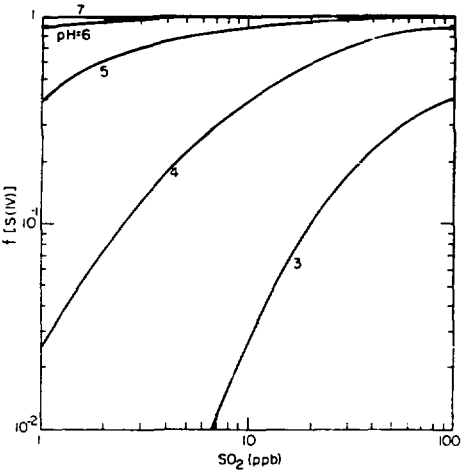

Fig. 2. The effect of partial pressure of SO_2 on f[S(IV)] at pH of 7, 6, 5, 4, and 3. The f[S(IV)] is a function of S(IV) on which the aqueous oxidation rate of sulfites on soot particles depends. (XBL 808-5733)

In the oxidation of SO_2 by HNO_2 in water droplets, many concurrent and consecutive chemical reactions can occur as a result of the interaction between the nitrous acid and the sulfurous acid.[4-6] Hydroxylamine disulfonate (HADS) is the first stable product under most atmospheric conditions:

$$HNO_2 + 2HSO_3^- \rightarrow HNO(SO_3)_2^{-2} + H_2O \ .$$

The formation kinetic of HADS has been found to consist of three concurrent processes. The reaction rate law can be expressed as:

$$\frac{d[HADS]}{dt} = k_0[H^+]^2[NO_2^-] + k_I[H^+][NO_2^-][HSO_3^-] + k_{II}[NO_2^-][HSO_3^-]^2, \qquad (2)$$

where $k_0 \approx 8\times10^5$ l^2/mol-s (at 295K),

$k_I = 3.7\times10^{12}\ e^{-6100/T}$ l^2/mol^2-s, and

$k_{II} = 9.0\times10^{-4}\ e^{2.1(\mu)^{1/2}}$ l^2/mol^2-s,

T = temperature in Kelvin, and

μ = ionic strength in mol/l).

We tentatively assumed that this rate law will still hold in an atmosphere where concentrations of both nitrite and sulfite are several orders of magnitude lower than the concentrations used when this rate equation was derived.

HADS can undergo further reaction, either hydrolysis or sulfonation. Hydrolysis of HADS[7] produces hydroxylamine monosulfonate (HAMS) and sulfates. Sulfonation of HADS[8,9] yields amine trisulfonate. The major fraction of HADS undergoes hydrolysis under most atmospheric conditions.

HAMS can either undergo further hydrolysis to form hydroxylamine and sulfates or react with nitrous acid to produce nitrous oxide and sulfates. Although a complete rate law has not been determined for both reactions, the kinetic studies[7,10] indicate tha the reaction with nitrous acid is much more important than the hydrolysis. Therefore, it appears that the reaction between SO_2 and HNO_2 in atmospheric water droplets will first produce HADS, which undergoes acid-catalyzed hydrolysis to form HAMS and sulfate. HAMS then reacts with nitrous acid and finally becomes nitrous oxide and sulfate. The total stoichiometric equation can be expressed as

$$2HNO_2 + 2HSO_3^- \rightarrow N_2O\uparrow + 2HSO_4^- + H_2O.$$

If the reaction is at steady-state condition, then 1 mol of sulfate will be produced for every mole of SO_2 or HNO_2 consumed, assuming that the reaction rate between HAMS and nitrous acid is very large.

Comparison of Sulfate Production Mechanisms

We have carried out a box-type calculation to compare the relative importance of sulfate production mechanisms by soot particles and nitrous acid with other mechanisms involving liquid water. The following initial conditions were used in the calculation: liquid water, 0.05 g/m^3; SO_2, 0.01 ppm; O_3, 0.05 ppm; NH_3, 5 ppb; and CO_2, 0.000311 atm. Concentrations of particulate Fe and Mn of 250 ng/m^3 and 20 ng/m^3 respectively were assumed. However, only 0.13% of the total iron and 0.25% of the Mn are water soluble, according to Gordon et al.[11] The concentrations of soot and HNO_2 were taken as 10 μg/m^3 and 8 ppb respectively. The latter corresponds to 25 ppb of NO and 50 ppb of NO_2 at equilibrium conditions.[12]

The results of this calculation, shown in Figure 3, indicate that O_3, soot, and HNO_2 can be important mechanisms for sulfate aerosol formation. In general the O_3 mechanism is more important under high pH and/or photoactivity conditions when the concentration of O_3 is high, whereas both soot and HNO_2 processes are more important when the lifetime of fog or clouds is long[13] and the pH of the droplets is low. Both soot and HNO_2 processes can be dominant processes close to sources and in heavily polluted urban areas, where the concentrations of soot and NO/NO_2 are high and the pH of aqueous droplets is low.

PLANNED ACTIVITIES FOR FY 1981

We will calculate the concentration profile of all important species produced in NO_x/SO_2/liquid/H_2O systems as a function of reaction time.

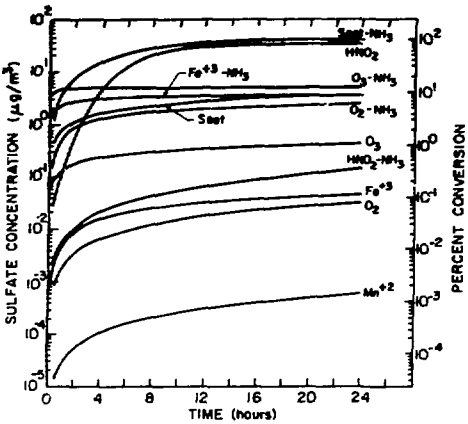

Fig. 3. Comparison of the relative importance of various sulfate production mechanisms involving liquid water based on a box-type calculation. (XBL 808-5735)

REFERENCES

1. S. G. Chang, R. Brodzinsky, R. Toossi, S. S. Markowitz, and T. Novakov, "Catalytic Oxidation of SO_2 on Carbon in Aqueous Suspensions," Proceedings, Conference on Carbonaceous Particles in the Atmosphere, Lawrence Berkeley Laboratory report LBL-9037, 1979, p. 122.

2. R. Brodzinsky, S. G. Chang, S. S. Markowitz, and T. Novakov, "Kinetics and Mechanism for the Catalytic Oxidation of Sulfur Dioxide on Carbon in Aqueous Suspensions," Journal of Physical Chemistry, vol. 84, 1980, p. 3354.

3. S. B. Oblath, S. S. Markowitz, T. Novakov, and S. G. Chang, "Kinetics of the Formation of Hydroxylamine Disulfonate by Reaction of Nitrite with Sulfites," Journal of Physical Chemistry, vol. 85, 1981, p. 1017.

4. F. Raschig, Schwefel und Stickstoffstudien (Berlin: Verlag Chemie, 1924).

5. W. Latimer and J. H. Hildebrand, Reference Book of Inorganic Chemistry (New York: Macmillan, 1951), p. 208.

6. W. Duecker and J. West, eds., The Manufacture of Sulfuric Acid, American Chemical Society, Washington, D.C., Monograph Series No. 144, 1959.

7. S. Naiditch and D. M. Yost, "The Rate and Mechanisms of the Hydrolysis of Hydroxylamine Disulfonate Ion," Journal of American Chemical Society, vol. 63, 1941, p. 2123.

8. S. Yamamoto and T. Kaneda, "Kinetics of Formation of Hydroxylamine Disulfonate and Nitrilosulfonate by Raschig's Hydroxylamine Process," Nippon Kagaku Zasshi, vol. 80, 1959, p. 1098.

9. V. S. Seel and H. Knorre, "Die Umsetzung von Nitrit mit Hydrogensulfit in Hydrogensulfit-sulfit-pufferlosungen," Zeitschrift für Anorganische und Allegemeine Chemie, vol. 313, 1961, p. 70.

10. V. F. Seel and H. Pauschmann, "Zum Kinetic der Umsetzung von Hydroxylaminemonosulfonat mit Nitrit," Zeitschrift für Naturforschung, vol. 17b, 1962, p. 347.

11. G. E. Gordon, D. D. Davis, G. W. Israel, H. E. Landsberg, and T. C. O'Haver, Atmospheric Impact of Major Sources and Consumers of Energy, NSF/RA/E-75/189 (1975). Available from NTIS as PB 262 574.

12. S. E. Schwartz and W. H. White, Equilibrium Solubility of the Nitrogen Oxides and Oxyacids in Aqueous Solution, Brookhaven National Laboratory Report BNL27102, Long Island, N.Y., 1980.

13. R. Toossi, S. G. Chang, and T. Novakov, "Lifetime of Liquid Water Drops in Ambient Air: Consideration of the Effects of Surfactants and Chemical Reactions," in Atmospheric Aerosol Research Annual Report 1977-78, Lawrence Berkeley Laboratory report LBL-8696, 1979, p. 149.

KINETICS OF THE REACTION BETWEEN NH_2OH AND SO_2 IN AQUEOUS SOLUTIONS*

S. Gomiscek, R. Clem, T. Novakov, and S. Chang

INTRODUCTION

Hydroxylamine, one of the species produced as a result of interaction between NO_x and SO_2 in aqueous solution can undergo further reaction[1-3] with SO_2 to form either sulfuric acid or ammonium bisulfate. We have investigated the kinetics of this latter reaction as part of an effort to understand the importance of the interaction of NO_x with SO_2 in atmospheric aqueous droplets in terms of acid rain and sulfate aerosol formation.

ACCOMPLISHMENTS DURING FY 1980

The reaction mixture was prepared by aliquoting to a 100-ml volumetric flask in the following sequence: hydroxylamine stock solution, buffer solution, and finally sodium bisulfite. The flask was quickly made to volume with the distilled water after the last addition and mixed; then the first polarographic determination of the hydroxylamine concentration was made. Subsequent measurements were made after the appropriate time intervals to monitor the time rate of hydroxylamine disappearance. For some of the work the solutions were thermostatted.

The first set of experiments determined the reaction order with respect to total hydroxylamine. An excess of bisulfite was used, and the solution was buffered at pH 5 in these runs. Figure 1 shows a semilog plot of total hydroxylamine concentration versus time for several initial concentrations. Parallel lines indicate a first order dependence on hydroxylamine.

The dependence of the reaction on total sulfite was determined by varying the excess sulfite concentration for a fixed hydroxylamine concentration at pH 5. Because the hydroxylamine is first order as determined above, one can write the rate law as

$$\frac{-d[\text{total hydroxylamine}]}{dt} = k_{obs}[\text{total hydroxylamine}]\cdot[\text{total sulfite}]^n,$$

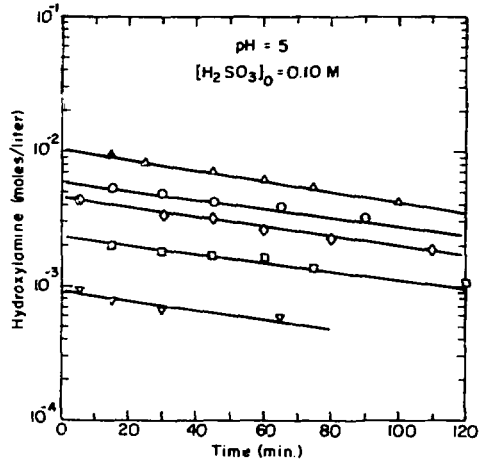

Fig. 1. Loss of hydroxylamine as a function of time. Straight lines indicate first order dependence. $[H_2SO_3]$ indicates total sulfite, (S(IV) concentration. (XBL 809-5897)

in which one can define

$$Q = -\frac{d\ln[\text{total hydroxylamine}]}{dt} = k_{obs}[\text{total sulfite}]^n.$$

A log-log plot of Q versus [total sulfite] should give a straight line with the slope equal to the order of the reaction with respect to total sulfite. Figure 2 shows that the slope is 0.94, which is regarded as first order dependence. Therefore, the reaction follows the rate law

$$-\frac{d[\text{total hydroxylamine}]}{dt} = k_{obs}[\text{total hydroxylamine}]\cdot[\text{total sulfite}].$$

The rate of reaction was found to be independent of the ionic strength of the solution. The rate constant k_{obs} in 1/mol-s was determined at two temperatures: 7.67×10^{-3} at 35°C and 1.48×10^{-3} at 22°C. Sisler and Audrieth[1] and Fraser[3] suggested that formation of both sulfamic acid and ammonium bisulfate involves attack by the $SO_2 \cdot H_2O$ on the NH_2OH. The reaction can therefore be expressed as

*This work was supported by the Assistant Secretary for Environment, Office of Health and Environmental Research, Division of Biomedical and Environmental Research, U.S. Department of Energy under Contract No. W-7405-ENG-48 and by the Morgantown Energy Research Center under Contract No. AA 050515.

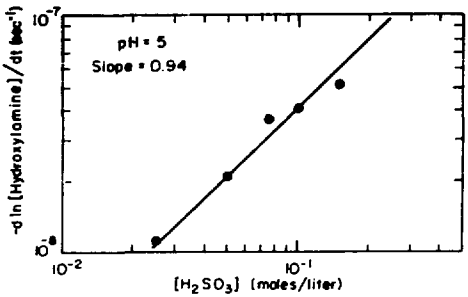

Fig. 2. Dependence of the rate on total sulfite concentration. The slope is the order of the reaction with respect to sulfite. (XBL 809-5898)

$$NH_2OH + SO_2 \cdot H_2O \xrightarrow{k_a} NH_2HSO_3 + H_2O$$
$$NH_2OH + SO_2 \cdot H_2O \xrightarrow{k_b} NH_4HSO_4$$

The rate law can be written as

$$-\frac{d[\text{total hydroxylamine}]}{dt} = (k_a + k_b)[NH_2OH][SO_2 \cdot H_2O] . \quad (2)$$

To evaluate the rate constant and activation energy of both reactions using our experimental measurements, Equation (1) is expressed in terms of the concentration of reaction species NH_2OH and $SO_2 \cdot H_2O$. Because [total hydroxylamine] = $[NH_2OH] + [NH_3OH^+]$ and [total sulfite] = $[SO_2 \cdot H_2O] + [HSO_3^-] + [SO_3^=]$, Equation (1) can be written as

$$-\frac{d[\text{total hydroxylamine}]}{dt} = k_{obs}\left(1 + \frac{[H^+]}{K_n}\right)$$

$$\left(1 + \frac{K_1}{[H^+]} + \frac{K_1K_2}{[H^+]^2}\right) \cdot [NH_2OH][SO_2 \cdot H_2O] . \quad (3)$$

where K_n, K_1, and K_2 are respectively the acid dissociation constant for hydroxylamine and the first and second dissociation constants for sulfurous acid.

By comparing Equations (3) and (4), we obtain the following relationship:

$$k_a + k_b = k_{obs}\left(1 + \frac{[H^+]}{K_n}\right)\left(1 + \frac{K_1}{[H^+]} + \frac{K_1K_2}{[H^+]^2}\right). \quad (4)$$

The ratio k_a/k_b can be obtained by the corresponding ratio of the products $[NH_2HSO_3]/[NH_4HSO_4]$; this ratio was determined by Fraser[3] at several temperatures. The following values, obtained from the interpolation of Fraser's result were used: 9 at 22°C and 19 at 35°C. By applying the transition-state theory,[4] the enthalpy and entropy of activation for the formation of both sulfamic acid and ammonium bisulfate can be calculated as shown in Table 1. The results of this study are in fairly good agreement with those of Fraser.

PLANNED ACTIVITIES FOR FY 1981

We will study the kinetics of other reactions involved in the interaction of NO_x and SO_2 in aqueous solution.

REFERENCES

1. H. H. Sisler and L. F. Audrieth, "The Preparation of Sulfamic Acid by the Hydroxylamine-Sulfur Dioxide Reaction," Journal of the American Chemical Society, vol. 61, 1939, p. 3389.

2. D. S. Brackman and W. C. E. Higginson, "The Reaction Between Hydroxylamine and Sodium Sulphite in Solution in Dilute Acid," Journal of the Chemical Society, London, 1953, p. 3896.

3. R. T. M. Fraser, "The Hydroxylamine-Sulphur Dioxide Reaction," Journal of the Chemical Society, London, 1965, p. 1747.

4. S. W. Benson, The Foundations of Chemical Kinetics, New York: McGraw-Hill, 1960.

Table 1. The enthalpy and entropy of activation for the formation of sulfamic acid and ammonium bisulfate by the reaction of NH_2OH with $SO_2 \cdot H_2O$.

	Sulfamic acid		Ammonium bisulfate	
	$\Delta H_a^\ddagger$ (kcal/mol)	$\Delta S_a^\ddagger$ (e.u.)*	$\Delta H_b^\ddagger$ (kcal/mol)	$\Delta S_b^\ddagger$ (e.u.)
Fraser	10.9	-16	1	-56
This work	13.4	- 6.1	3.0	-45.8

*e.u. = entropy units.

THE ROLE OF FLY ASH IN THE CATALYTIC OXIDATION OF SO_2*

S. Cohen, S. Chang, S. Markowitz, and T. Novakov

INTRODUCTION

The catalytic behavior of fly ash in the oxidation of S(IV) in aqueous systems has been reported.[1,2] Prior work has considered the potential of fly ash as a scrubber medium,[1-3] and has suggested that fly ash may function in promoting acid rain formation in droplets.[4] Although several properties of the ash--surface characteristics, metal oxide content, trace metal dissolution--have been proposed to account for its catalytic role, no systematic investigation of the nature of the catalysis has been made. It is important to distinguish between surface and homogeneous catalysis. For example, the presence of chelating agents in wet scrubbers containing fly ash should inhibit catalysis by leached metals.[1,5]

In this study the oxidation of S(IV) in slurries of fly ash has been examined after different ash pretreatment and under varying experimental conditions. Our evidence indicates that dissolved iron is a prime factor in fly-ash-catalyzed oxidation of SO_2.

ACCOMPLISHMENTS DURING FY 1980

Materials and Methods

Mallinckrodt or Baker reagent-grade chemicals were used without further purification. The fly ash types were National Bureau of Standards (NBS) Standard Reference Material 1433a, and four lot samples, referred to as A-D, were used. A is from the TVA Shawnee Power Plant; B is from the Duke Power Steam Plant; C is from the Jim Bridger Plant in Wyoming; and D is an untreated ash sample obtained from Lawrence Livermore Laboratory.

Reactions were monitored by three different methods:

1. in open-air Erlenmeyer flasks agitated with a magnetic stirrer, and with S(IV) loss being monitored by idometry;

2. the reaction was set up as above, except that SO_3^{2-} loss and SO_4^{2-} appearance monitored by ion chromatography; and

3. in a closed system--allowing no diffusion of O_2 into solution during the course of the reaction--with O_2 decay from initially saturated solutions being monitored with a Clark-type O_2 electrode.

The initial S(IV) concentration in the reactions studied varied from 9.0×10^{-4} to 1.5×10^{-2} M. The pH varied from 2.5 to 3.9 by using appropriate mixtures of $H_2O \cdot SO_2$ and $Na_2S_2O_5$. The fly ash concentration was varied from 0.10% to 0.36% by weight. Although reproducibility was at times inadequate, most rates reported are the average of 2-3 runs agreeing within 10%.

Leaching experiments are described elsewhere.[7]

Equipment and Materials

Elemental and chemical compositions of fly ash were characterized by ion chromatography and atomic absorption (AA). AA work was performed on a Perkin-Elmer Model 360 atomic absorption instrument in an air-acetylene or N_2O-acetylene flame. The ion chromatograph used was a Dionex System 14 equipped with precolumn and, where necessary, a concentrator column. A 0.22-μm pore size Millipore filter was used to filter solutions for leachate analysis and reaction aliquots. This pore size was chosen as the maximum size which appears to trap all ash particles to which metals might adsorb.[7]

Role of Surface in Catalysis

To determine the relative importance of surface-mediated or solution-phase reactions, a reaction slurry was filtered after the reaction was partially complete. Loss of sulfite was monitored in the filtrate; and as can be seen in Figure 1, the reaction rate is not affected by removing particulate matter.

Because the catalysis is apparently due to trace metals which can be leached from the ash, an attempt was made to remove such species from the ash surface by leaching with different solvents. Leaching with deionized water or strongly basic solution did not affect the ash reactivity. However, an acid wash in 0.02 N acid completely deactivated the ash. Metals commonly implicated in SO_2 oxidation--Cu, Fe, Mn, Co, V--could be removed by an acid wash, depending on chemical state, so it is not surprising that washing with acid deactivates the fly ash.

Leaching experiments were carried out using a variety of solvents. In Table 1 an attempt has been made to correlate Fe and Mn concentrations with ash reactivity. These are the only two catalysts present in high enough concentration to account for the observed rates. Fe concentration shows a good correlation with reaction rates (Table 1). The fact that the reaction reaches its maximum rate within 3-4 min of initiation indicates that the species responsible for the catalysis is rapidly leached from the ash and is therefore found on the surface, rather than in the aluminosilicate matrix. V, Co, Cu, and Mn are present to some

*This work was supported by the Assistant Secretary for Environment, Office of Health and Environmental Research, Division of Biomedical and Environmental Research of the U.S. Department of Energy under Contract No. W-7405-ENG-48 and by the Morgantown Energy Research Center under Contract No. AA 050515.

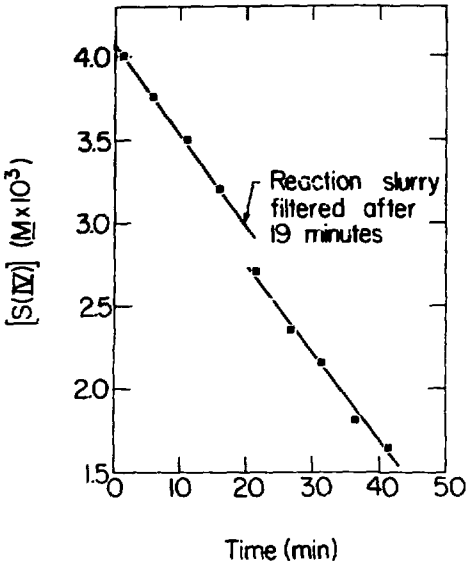

Fig. 1. Comparison of rate of [S(IV)] oxidation before and after filtering reaction slurry. Initial pH = 2.9, ["D" fly ash] = 0.18%. (XBL 809-1927)

degree on the ash surface, whereas Fe is predominantly matrix-associated.[8] Since significant concentrations of Fe are present in stirred reaction slurries, we believe that the small quantity of Fe which is surface-associated--perhaps as a ferrous or ferric salt--is catalytically important.

By augmenting the catalyst concentration, we hoped to increase the reaction rate. Stirring reaction slurries for long time periods to increase the Mn and Fe concentrations by as much as twofold did not always increase the reaction rate. Graefe et al.[1] also observed this phenomenon. In addition, there was no simple relation between fly ash concentration and reaction rate: Although increasing the ash content in reaction slurries generally accelerated the reaction, the rate dependence on fly ash concentration was not monotonically increasing and not reproducible with varying reaction conditions. Equilibrium control of metal dissolution could be responsible for this behavior. This would be independent of kinetic control of the leaching described in the preceding paragraph. Chemical kinetic saturation is another possibility. Hudson found a zero order dependence on Fe concentration for [Fe] > 1 ppm.[9]

pH Studies

It is important to know the pH dependence of the reaction for at least two reasons: The two opposing factors which are controlled by pH are (1) metal dissolution (favored at lower pH), and (2) fraction of SO_3^{2-} and HSO_3^- present relative to the total concentration of S(IV) species (increases with increasing pH). Many studies implicate $SO_3^=$ as the reactive species in catalytic oxidation of S(IV).[11,12] The U-shaped curve in Figure 2 is thus qualitatively what is expected for homogeneous catalysis by metals leached from the ash.

Comparison With Known Rates

Attempts were made to correlate reaction rates observed here with values in the literature for metal-assisted S(IV) oxidation.[11-16] Initial rates of the fly ash reaction were compared to initial rates calculated from the referenced equations. For each case, the concentration of metal catalyst used was the maximum found in a fly

Table 1. Comparison of rates with metal concentrations.

	[Metal] in $NH_2OH \cdot HCl$ Extract[a]		[Metal] in Filtered Reaction Slurry[a]		Reaction Rate[b]	
Ash type	[Mn]	[Fe]	[Mn]	[Fe]	Reaction in Untreated Ash	In NH_2OH HCl Extracted Ash
NBS	0.071	1.8	<0.01	-	1.92×10^{-5}	-
A	0.64	12.5	0.05	1.9	12.0×10^{-5}	1.0×10^{-5}
B	1.71	5.0	0.19	1.2	3.6×10^{-5}	1.3×10^{-5}
C	0.59	7.2	0.07	1.5	8.0×10^{-5}	6.0×10^{-5}
D	0.83	3.4	0.11	-	6.8×10^{-5}	1.4×10^{-5}

[a]All metal concentrations are in μg/ml.

[b]Initial rate - d[S(IV)]/dt (mol/l min).

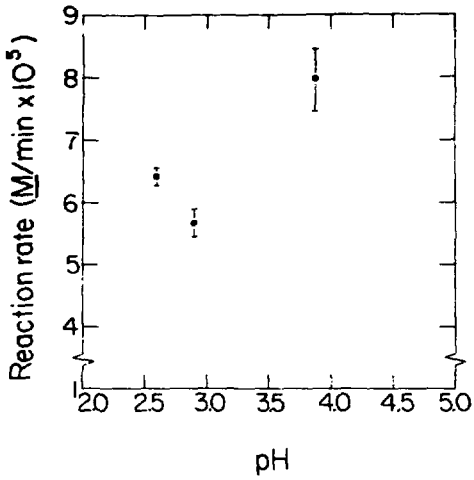

Fig. 2. pH dependence of fly ash (type D) reaction rate. pH variation during reaction = ± 0.05. $[S(IV)]_0 = 9 \times 10^{-3}$ M, [fly ash] = 0.12%, T = 22°C. (XBL 809-1928)

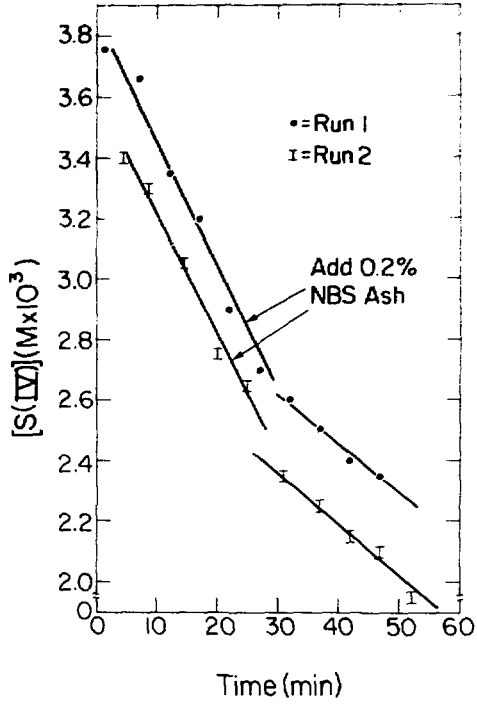

Fig 3. Demonstration of rate inhibition by NBS ash. Initial pH = 2.9 ± 0.1, ["D" fly ash] = 0.15%. (XBL 809-1926)

ash solution. As expected, Mn is not present in high enough concentration to account for the observed rate, whereas Fe is. Because of the complexity of the system, this result serves only to support the empirical evidence presented above.

Inhibition

Other complications exist. The presence of inorganic arsenite and SO_4^{2-} from the ash could inhibit the reaction.[10,18] Several organic compounds also inhibit the oxidation.[9,19] It was suspected that the NBS ash could be unreactive because of the presence of inhibitor in addition to the lack of catalyst. X-ray fluorescence and combustion data show the NBS ash contains more C and As than active ash type D. Inspection of Figure 3 shows that the NBS ash does indeed serve as an inhibitor. Extracting the NBS ash in base to remove suspected inhibitors arsenite and cyanide does not, however, render this ash more catalytically active. In addition, neither soxhlet extraction using methanol nor combustion to remove all organic matter causes a significant rate increase.

CONCLUSION

Fly ash is not a uniform substance. Compositional inhomogeneities are to be expected even within one sample lot. For this reason, a thorough rate study of fly-ash-catalyzed SO_2 oxidation could serve little purpose. The goal of this study has been to isolate fly ash components essential to SO_2 oxidation. Evidence presented here discounts the importance of the ash surface in this catalysis. Filtering the reaction slurry leaves the rate unchanged. Also, leaching under relatively mild conditions which should not change surface morphology renders the ash catalytically inactive. Unimportance of the ash surface is not surprising considering the low surface area (1-30 m^2/gm) of most fly ash. In addition, it appears that Fe plays a more important role than Mn in the oxidation. Since Mn is more soluble than Fe at pH levels found in droplets and wet scrubbers, this result is important.

PLANNED ACTIVITIES FOR FY 1981

The synergistic effect of metal ions in fly ash on the catalytic oxidation of SO_2 will be investigated.

REFERENCES

1. A. F. Graefe et al., Report to National Air Pollution Control Administration, NTIS #PB 196781, 1970.

2. P. Marrier and H. P. Dibbs, "The Catalytic Conversion of SO_2 to SO_3 by Fly Ash and the Capture of SO_3 by CaO and MgO," Thermochimica Acta, vol. 8, 1974, p. 155.

3. G. E. Gordon, D. D. Davis, G. W. Israel, H. E. Landsberg, and T. C. O'Haver, "Atmospheric Impact of Major Sources and Consumers of Energy," National Science Foundation Report NSF/RA/E-75/189 (NTIS #PB 262574), 1975.

4. J. B. Green, Potential of Humic Acid as Stack Gas Scrubbing Media for Removal of Sulfur Dioxide and Fly Ash, Ph.D. dissertation, University of Maryland, 1977.

5. H. Head and S. C. Wang, EPA Alkali Scrubbing Test Facility Advanced Program, Basic Report, vol. 1, 1979.

6. S. Cohen et al., "Surface Characterization of Fly Ash," Atmospheric Aerosol Research Annual Report FY 80, Lawrence Berkeley Laboratory report LBL-10735, 1980, p. 37.

7. G. L. Fischer et al., "Filtration Studies with Neutron Activated Coal Fly Ash," Environmental Science and Technology, vol. 13, 1979, p. 689.

8. L. D. Hansen and G. L. Fisher, "Elemental Distribution in Coal Fly Ash Particles," Environmental Science and Technology, vol. 14, 1980, p. 1111.

9. J. L. Hudson, Sulfur Dioxide Oxidation in Scrubber Systems, Environmental Protection Agency report EPA-600/7-80-083, 1980.

10. M. J. Matteson, W. Stober, and H. Luther, "Kinetics of the Oxidation of Sulfur Dioxide by Aerosols of Manganese Sulfate," Industrial and Engineering Chemical Fundamentals, vol. 8, 1969, p. 677.

11. H. Bassett and W. G. Parker, "The Oxidation of Sulphurous Acid," Journal of American Chemical Society, 1951, p. 1546.

12. L. A. Barrie and H. W. Georgii, "An Experimental Investigation of the Absorption of Sulphur Dioxide by Water Drops Containing Heavy Metal Ions," Atmospheric Environment, vol. 10, 1976, p. 743.

13. E. C. Fuller and R. H. Crist, "The Rate of Oxidation of Sulfite by Oxygen," Journal of American Chemical Society, vol. 63, 1941, p. 1644.

14. P. Brimblecombe and D. J. Spending, "The Catalytic Oxidation of Micromolar Aqueous Sulfur Dioxide - I," Atmospheric Environment, vol. 8, 1974, p. 937.

15. D. R. Coughanowr and F. E. Krause, "The Reaction of SO_2 and O_2 in Aqueous Solutions of $MnSO_4$," Industrial and Engineering Chemical Fundamentals, vol. 4, 1965, p. 61.

16. D. G. Karraker, "The Kinetics of the Reaction between Sulfurous Acid and Ferric Ion," Journal of Physical Chemistry, vol. 67, 1963, p. 871.

17. P.N. Dasgupta, private communication, August 1980.

18. L. C. Schroeter, Sulfur Dioxide: Application in Foods, Beverages, and Pharmaceuticals (Oxford: Pergamon Press, 1966), p. 56.

19. H. L. Backstrom, "The Chain-Reaction Theory of Negative Catalysis," Journal of Physical Chemistry, vol. 49, 1927, p. 1460.

SOOT IN THE ARCTIC*

H. Rosen, T. Novakov, and B. Bodhaine†

INTRODUCTION

Recent studies in the Arctic[1,2] show the presence of large aerosol concentrations that significantly affect optical transfer through the atmosphere and lead to the phenomenon of Arctic haze, which was first reported by Mitchell.[3] In particular, the observation of substantial concentrations of particulate sulfur and vanadium at the National Oceanographic and Atmospheric Administration and Geophysical Monitoring for Climatic Change sampling station near Barrow, Alaska, has attracted considerable attention.[1,2] Questions have been raised as to the anthropogenic character, sources, and climatic impacts of these aerosols. In order to gain a better understanding of these issues, a study of the physical and chemical properties of the carbonaceous aerosol at Barrow was initiated in October, 1979.

Recent studies of the urban aerosol indicate the presence of substantial graphitic carbon concentrations. These graphitic species--identified by a variety of modern analytical techniques (e.g., Raman spectroscopy,[4] photoacoustic spectroscopy,[5] thermal analysis[6])--are very effective absorbers of visible radiation and are responsible for the high optical absorption coefficients which have recently been observed in urban air.[7,8] The impacts of these highly absorbing particles on a regional or global scale have not been assessed so far, but they could be important, especially over regions with a high surface albedo like the polar icecaps. Furthermore, graphitic carbon can only be produced from combustion processes, and therefore it can offer a very attractive and convenient tracer for anthropogenic activity.

ACCOMPLISHMENTS DURING FY 1980

An aerosol sampler was constructed to collect parallel 47-mm quartz fiber and Millipore filter samples at a flow rate of ~1.5 cfm. The sampler had two chambers--a lower chamber which contained the pumps and an upper chamber for collecting the aerosol samples. The upper chamber was warmed by several thermostatically controlled heat lamps, while temperature control in the lower chamber was achieved by using a thermostatically controlled fan and heat lamps. The exhaust of the pumps was vented below the sampling platform. To minimize local contamination, the aerosol sampler was controlled by a wind sensor built by the University of Rhode Island group.[1] This allowed samples to be collected only when the wind was from the clean air sector at Barrow, between 0° N and 130° SE. Results obtained with and without the wind controller suggest that there is no significant influence from local sources. Approximately 50 filter pairs have been collected at sampling time intervals ranging from 2 days to 1 week. The quartz filters were used to determine the total carbon content of the aerosol by a combustion method,[9] and the Millipore substrate was used to determine the optical absorption coefficient of the aerosol by the LBL laser transmission method described elsewhere.[4,5,8] The absorption coefficients reported here are consistent with the optical constants of graphitic carbon and are expected to have an accuracy of better than a factor of two. The Millipore substrate was also analyzed by the X-ray fluorescence technique to determine the concentration of elements with $Z > 11$. The quartz blanks had a carbon loading of $< 0.5\ \mu g/cm^2$, while typical filter deposits corresponded to $15\ \mu g/cm^2$. Selected filters have been analyzed by Raman spectroscopy, thermal analysis, and solvent extraction techniques. The results of these analyses are described below.

Raman spectroscopy is a highly selective method of analysis which has been used to identify large concentrations of graphitic carbon in urban particulates.[4] This technique has been applied to the analysis of several samples collected at Barrow. The experimental arrangement and methods are described elsewhere.[4] The results are shown in Figure 1, in which the spectrum of an Arctic sample collected in December 1979 is compared to that of urban particulates, various source emissions, and carbon black. All these spectra show the presence of two intense Raman modes located at 1350 cm^{-1} and 1600 cm^{-1}, which have been identified as due to phonons propagating within graphitic planes.[10] This result shows that graphitic structures similar to carbon black and due to combustion processes are present in the Arctic aerosol. Furthermore, the high intensity in these modes indicates that, just as in urban samples, the graphitic structures represent a major component of the aerosol.

The filters collected at Barrow from Fall through late Spring have a grey or black appearance similar to that found for urban particulates. For the urban samples, this optically absorbing component has been identified as graphitic carbon.[4] Preliminary measurements on a limited number of samples show that the optically absorbing species in the Arctic has a $1/\lambda$ wavelength dependence, is

---

*This work was supported by the Assistant Secretary for Environment, Office of Health and Environmental Research, Division of Biomedical and Environmental Research of the U.S. Department of Energy under Contract No. W-7405-ENG-48 and by the National Science Foundation under Contract No. ATM 80-13707 and by the Air Resources Laboratory of the National Oceanographic and Atmospheric Administration.

†Geophysical Monitoring for Climatic Change Program of the Air Resources Laboratory, National Oceanographic and Atmospheric Administration, Boulder, Colo.

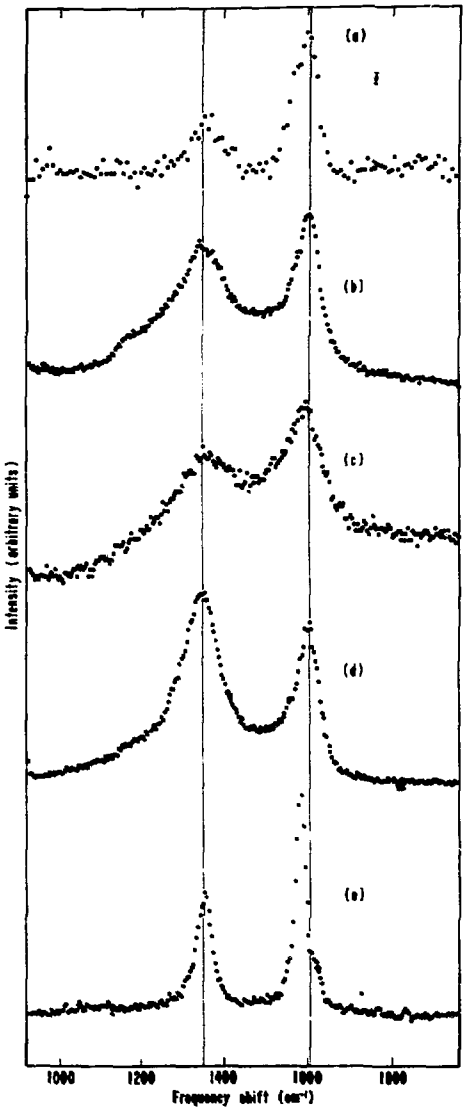

Fig. 1. Raman spectrum of an Arctic sample compared to those of urban particulates for various source emissions, carbon black, and polycrystalline graphite. (XBL 767-3091A)

insoluble in a wide range of solvents, and has a high temperature stability with an oxidation threshold of approximately 500°C. These results are consistent with the properties of graphitic carbon and strongly suggest that indeed the optically absorbing species at Barrow is graphitic in nature.

The seasonal variation of the optical absorptivity (or graphitic carbon concentration) of the Barrow aerosol is shown in Figure 2. The absorption coefficient changes by more than an order of magnitude from mid-October to early January and remains at a relatively high level throughout most of February, March, and April. It decreases substantially in May. The magnitude of the absorption coefficient during the Winter and Spring is comparable to that found in urban environments (Table 1) (i.e., the peak values in February are only about a factor of ten less than the average absorption coefficients in New York City and a factor of three less than those found in Berkeley, Calif., and Denver, Colo.). This absorption coefficient is large enough to produce significant optical effects. For example, an absorption coefficient of 5×10^{-6} m^{-1} extended over a path length of 10 km would produce an optical thickness of .05. This would be a large perturbation on the transfer of optical radiation through the atmosphere when the sun's irradiance is at a high level, as it is during part of these pollution episodes. In order to assess the importance of these effects, more detailed measurements of the seasonal variation in the optical properties (visible and infrared) and the vertical and horizontal extent of the aerosols need to be determined.

The pollution episodes observed at Barrow are not a local phenomenon but appear to be areawide with similar seasonal variations occurring at widely spaced sites across the Arctic.[11,12] This is illustrated in Figure 3, in which a comparison of the monthly variations in the blackness of the filter deposits collected at Barrow and Mould Bay, Canada, are shown. (The samples from Mould Bay were provided by Dr. L. A. Barrie and Dr. P. Hoff of the Canadian Atmospheric Environment Service.) These sampling stations are widely separated, yet the initial onset and duration of the episodes observed at these two sites are almost identical.

Using the optical constants of graphitic carbon determined from our urban studies,[13] we can make an estimate of the graphitic carbon

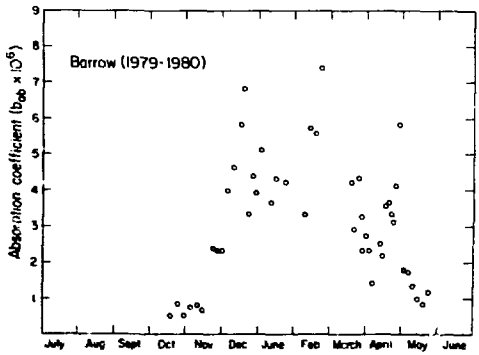

Fig. 2. Seasonal variations in the optical absorption coefficient in m^{-1} at Barrow from October 1979 to May 1980. (XBL 8010-4418)

Table 1. A comparison of absorption coefficients, carbon concentrations, and graphitic carbon concentrations at Barrow, Alaska, and various urban locations.

Site	Date	Number of Samples	Average Absorption Coefficient x 10^5 (M^{-1})	Average Total Carbon ($\mu g/m^3$)	Average Graphitic Carbon as Percent of Total Carbon[a]
Barrow, Alaska	12/79-4/80	33	.4	1.2	24
Argonne, Illinois	1/79-3/80	438	2.8	8.1	22
Gaithersburg, Maryland	1/79-3/80	381	2.1	6.1	22
Denver, Colorado	11/78-5/79	141	2.4	9.8	16
Anaheim, California	8/77-1/80	852	4.9	16.6	19
Fremont, California	7/77-3/80	924	3.4	12.0	18
Berkeley, California	6/77-4/80	998	2.1	6.7	20
New York, New York	11/78-4/80	439	6.4	15.2	27

[a]Calculated from optical constants in Reference 13.

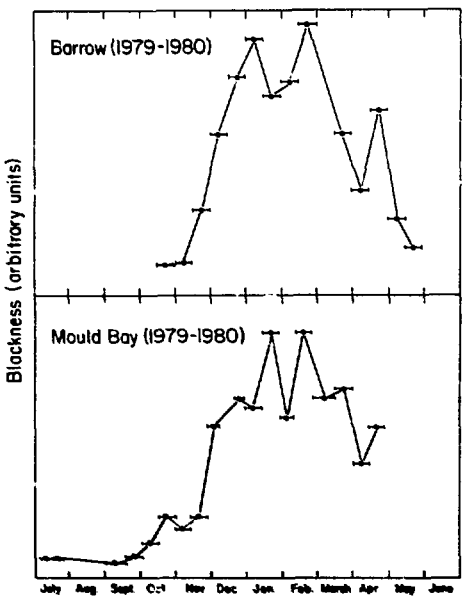

Fig. 3. A comparison between the seasonal variation in the blackness of filter deposits collected at Barrow, Alaska, and Mould Bay, Canada, in 1979 and 1980. Mould Bay samples were provided by L. A. Barrie and P. Hoff of the Canadian Atmospheric Environment Service. (XBL 801C-4420)

concentration at Barrow. These results are shown in Figure 4, where we plot the graphitic carbon concentration as a fraction of the total carbon content of the aerosol for various periods of time during the year. The results shown a strong enrichment of the graphitic fraction of the carbonaceous aerosol from early to late winter. The concentration of graphitic carbon in late February is almost 40% of the carbonaceous mass. It is remarkable that this percentage is higher than that found in urban centers like New York City and Los Angeles.[14] After its peak in February, the fraction of graphitic carbon seems to level off to a value which is more typical of those found in urban environments. The interpretation of these interesting features in terms of transport, atmospheric chemistry, and deposition processes is complicated and will have to await more detailed analyses and further measurements.

In summary, these observations indicate that large graphitic concentrations can develop at remote locations. If one ignores the possible contribution of natural burning processes (e.g., forest fires), which is expected to be small during these times of year in the northern hemisphere, this component can be attributed directly to the burning of fossil fuels. The source and the climatic effects of these highly absorbing species are uncertain and will have to await more systematic measurements and careful modelling.

PLANNED ACTIVITIES FOR FY 1981

The project will continue to explore the sources and climatic impact of carbonaceous aerosols in the Arctic region.

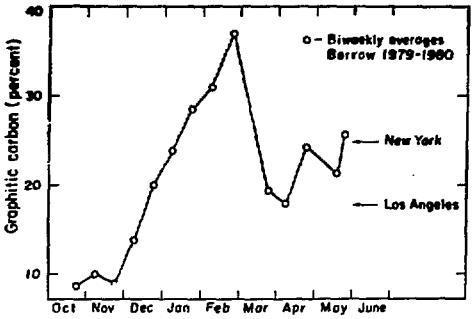

Fig. 4. Seasonal variation of graphitic carbon as a percentage of the total carbon content of the aerosol at Barrow from October 1979 to May 1980. These values are compared to the average values obtained in New York City and Los Angeles. (XBL 809-2013)

ACKNOWLEDGMENTS

The authors would like to acknowledge stimulating ahd helpful discussions with Lester Machta, National Oceanographic and Atmospheric Administration, and with Michael MacCracken, Lawrence Livermore Laboratory.

REFERENCES

1. K. A. Rahn and R. J. McCaffrey, "On the Origin and Transport of the Winter Arctic Aerosol," Proceedings, Conference on Aerosols: Anthropogenic and Natural - Sources and Transport (New York City: New York Academy of Sciences, January 9-12, 1979, in press).

2. G. E. Shaw and K. Stamnes, "Arctic Haze: Perturbation of the Polar Radiation Budget," Proceedings, Conference on Aerosols: Anthropogenic and Natural - Sources and Transport (New York City, New York Academy of Sciences: January 9-12, 1979, in press).

3. M. Mitchell, "Visual Range in the Polar Regions with Particular Reference to the Alaskan Arctic," Journal of Atmospheric Terrestrial Physics, Special Supplement, 1956, pp. 195-211.

4. H. Rosen, A. D. A. Hansen, L. Gundel, and T. Novakov, "Identification of the Optically Absorbing Component in Urban Aerosols," Applied Optics, vol. 17, 1978, p. 3859.

5. Z. Yasa, N. M. Amer, H. Rosen, A. D. A. Hansen, and T. Novakov, "Photoacoustic Investigation of Urban Aerosol Particles," Applied Optics, vol. 18, 1979, p. 2528.

6. R. Dod et al., "Application of Thermal Analysis to the Characterization of Nitrogenous Aerosol Species," Energy and Environment Division Annual Report, 1979, Lawrence Berkeley Laboratory report, LBL-10735, 1980.

7. R. E. Weiss, A. P. Waggoner, R. Charlson, D. L. Thorsell, J. S. Hall, and L. A. Riley, "Studies of the Optical, Physical, and Chemical Properties of Light Absorbing Aerosols," Proceedings, Conference on Carbonaceous Particles in the Atmosphere, Lawrence Berkeley Laboratory report LBL-9037, 1979, p. 257.

8. M. Sadler, R. J. Charlson, H. Rosen, and T. Novakov, An Intercomparison of the Integrating Plate and the Laser Transmission Methods for Determination of Aerosol Absorption Coefficients, Lawrence Berkeley Laboratory report LBL-11176, 1980.

9. P. K. Mueller, R. W. Mosley, and L. B. Pierce, "Carbonate and Non-carbonate Carbon in Atmospheric Particulates," Second International Clean Air Congress, Proceedings (New York Academic Press, 1971).

10. F. Tuinstra and J. L. Koenig, "Raman Spectrum of Graphite," Journal of Chemical Physics, vol. 53, 1970, p. 1126.

11. L. A. Barrie et al., "The Influence of Mid-Latitudinal Pollution Sources in the Haze in the Canadian Arctic," Atmospheric Environment (in press).

12. B. Ottar et al., "The Transfer of Airborne Pollutants to the Arctic Region," Atmospheric Environment (in press).

13. A. D. A. Hansen et al., "The Use of an Optical Attenuation Technique to Estimate the Carbonaceous Component of Urban Aerosols,' Energy and Environment Division Annual Report, 1979, Lawrence Berkeley Laboratory report LBL-10735, 1980, p. 16.

14. H. Rosen, A. D. A. Hansen, R. L. Dod, and T. Novakov, "Soot in Urban Atmospheres: Determination by an Optical Absorption Technique," Science, vol. 208, 1980, p. 741.

AN INTERCOMPARISON OF THE INTEGRATING PLATE AND THE LASER TRANSMISSION METHODS FOR DETERMINATION OF AEROSOL ABSORPTION COEFFICIENTS*

M. Sadler,† R. Charlson,† H. Rosen, and T. Novakov

INTRODUCTION

Recent studies of atmospheric aerosol particles indicate the presence of a large, optically absorbing component which can cause both visibility degradation and climatic effects. The nature of this absorbing species has been investigated in the past by solvent extraction, heat treatment, and wavelength dependence studies.[1,2] These investigations led to the conjecture that it could be a graphite-like material. More recently, the Raman scattering technique has been applied to identify this component in urban aerosols on a microscopic level as "graphitic" carbon.[1]

The fact that aerosol particles absorb light is evident from the usual grey or black appearance of filter samples collected from even rural locations. However, the absolute measurement of the component of extinction due to absorption, σ_{ap}, has posed significant challenges. Here we define the extinction coefficient, σ_{ext}, and its components with the Beer-Lambert law. For light of intensity I passing through an atmospheric path of length dx:

$$\frac{dI}{I} = -\sigma_{ext}dx = -(\sigma_{scatter} + \sigma_{absorption})\ dx$$

and

$$\sigma_{absorption} = \sigma_{absorption\ by\ particles} + \sigma_{absorption\ by\ gases} = \sigma_{ap} + \sigma_{ag}.$$

Not only is the measurement of σ_{ap} difficult, it is also extremely hard to make aerosols of known absorption coefficient for testing, calibration, and validation of methods.

Historically, one of the earliest measurements was performed by Waldram,[3] who measured the total extinction and its scattering component, arriving at the absorption component by subtraction. He found a relatively large percentage of extinction to be caused by particle absorption--typically half in an industrial area of England. However, this result has often been discounted as being atypical, and the assumption is usually that $\sigma_{ext} \cong \sigma_{scat}$.

There are fundamentally two general approaches in use for assessing light absorption by particles. One set of methods aims at establishing the absorption coefficient in the atmosphere, σ_{ap}; the other set of methods determines the imaginary refractive index of the bulk material of which the particles are formed. These approaches can be connected via Mie calculations if size distribution and the distribution of absorbing material with size are known.

In addition to the difference method of Waldram,[3] the integrating plate method,[4] the laser transmission method, and the multipass transmissometer[5] are examples of the first of these approaches; the integrating sphere,[6] the Kubelka-Monk method,[7] and inversion of angular scattering data have been used to estimate the imaginary refractive index of the material of which the particles are formed.

Two of these methods (the integrating plate and laser transmission) have been extensively used because of their practicality. This paper will compare the absorption coefficients determined by these two methods at a wide range of sites. Furthermore, these absorption coefficients will be correlated to the total carbon content of the aerosol. These measurements should provide an independent test of the strong correlation found by previous investigators[8,9] at urban locations, as well as to extend this type of observation to rural areas.

ACCOMPLISHMENTS DURING FY 1980

Five sampling sites in the western part of Washington state were used in this study, from a highly congested site in a highway tunnel to a very remote site on a western foothill in the Olympic Mountains. By sampling such diverse aerosol conditions, the range of absorption coefficients of the air samples was nearly four orders of magnitude, from $\sim 10^{-7}$ m^{-1} to 10^{-3} m^{-1}, with the total carbon concentration ranging from about 5 $\mu g/m^3$ (Mt. Octopus) to nearly 90 $\mu g/m^3$ (highway tunnel). The sites are shown in Figure 1.

The results of these comparisons are shown graphically in Figures 2 and 3. In Figure 2, a plot of absorption coefficients is shown, as determined by the Integrating Plate Method (IPM)

*This work was supported by the Assistant Secretary for Environment, Office of Health and Environmental Research, Division of Biomedical and Environmental Research of the U.S. Department of Energy under Contract No. W-7405-ENG-48 and by the National Science Foundation under Contract No. ATM 80-13707.

†Department of Civil Engineering, University of Washington, Seattle, Washington.

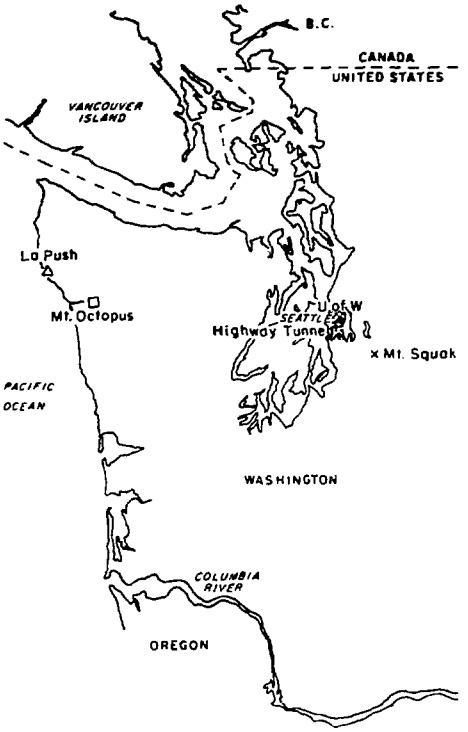

Fig. 1. Sampling sites. (XBL 811-7714)

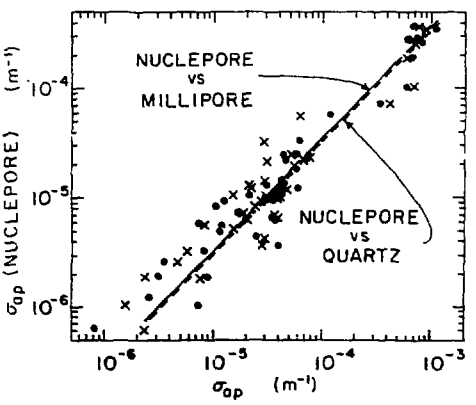

Fig. 2. Light absorption coefficient, $\sigma_{ap}(m^{-1})$, determined on Millipore (X) and quartz (O) filters. (XBL 811-7713)

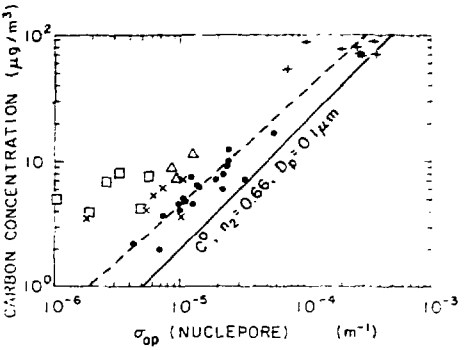

Fig. 3. Light absorption coefficient, $\sigma_{ap}(m^{-1})$ determined by the IPM versus total carbon concentration in μg/m^3. For site notation, see Figure 1. (XBL 811-7712)

using a Nuclepore substrate and the Laser Transmission Method (LTM) using a Millipore substrate. Also shown in the figure are absorption coefficients determined at the University of Washington on quartz fiber filters. A total of 44 filters of each type were used in this comparison. The correlation coefficient between the two measurements is 0.95, with the absorption coefficient determined by the LTM being greater by a factor of approximately 2.5 than the one determined by the IPM.

Figure 3 presents the plot of the concentration of total carbon (μg/m^3) versus the absorption coefficient from Nuclepore filters. The correlation found between these two variables was 0.90. Also shown in this figure is a value of σ_{ap} for monodisperse graphite particles (n_2 = 0.66, D_p = 0.1 μm), estimated as a function of mass concentration from Faxfog and Roessler.[10]

Three points emerged as the main conclusions of this study. First, the light absorption coefficients determined by these two methods are comparable and highly correlated. The reason for the higher indicated absorption coefficient using the LTM could be due to several factors, including (1) penetration effects in the Millipore substrate, which could lead to enhanced absorption due to multiple scattering effects within the filter medium itself; (2) possible pile-up at the holes or loss of particles in the holes of the Nuclepore substrate; (3) differences in the collection efficiency of the two substrates. Studies are under way in both of our laboratories to assess the magnitude of these effects. However, the differences found between these two techniques are small in comparison with the large uncertainties reported in the literature for the magnitude of the absorbing component of aerosol particles. These differences are also small compared to the range of more than three orders of magnitude observed in the value of σ_{ap}.

Second, and at least as important, a high degree of correlation is found between the absorption coefficients, σ_{ap}, and the carbon-loading

with the ratio of $[C]/\sigma_{ap}$ being similar at the highway tunnel, the University of Washington, and Mt. Squak. This correlation has been observed in the past[8,9] in many urban locations and for various source emissions, but this work represents the first verification of this important result by an independent absorption technique. Both these results are quite independent of site and are correspondingly independent to a high degree of the concentrations of carbonaceous material or level of σ_{ap}. The higher value of $[C]/\sigma_{ap}$ for the remote sites on the Olympic peninsula may be an indication of a very small natural background of non-light-absorbing carbon compounds. Such a background evidently might have values of total carbon of the order one to a few $\mu g/m^3$. The results also indicate that light-absorbing aerosols are ubiquitous in the atmosphere, even in such remote locations as our coastal sites. The fact that the ratio of $[C]/\sigma_{ap}$ is nearly the same in rural areas as in an urban area might imply that the light-absorbing carbonaceous materials in our rural samples were derived from an urban source. This suggestion is of course highly tentative and requires further measurements for resolution.

Third, we include in Figure 3 a comparison of the observed C concentration/σ_{ap} relationship to a calculation from the Mie formalism for pure graphite particles. Uncertainties of a factor of two or so exist in the imaginary refractive index for graphitic carbon, with 0.66 appearing as a typical value.[11] This calculated relationship is close to the observed values, which is consistent with the suggestion of Novakov[12] and Rosen et al.[9] that soot (which contains a graphitic and an organic component) is a major fraction of the carbonaceous aerosol in urban areas.

REFERENCES

1. H. Rosen, A. D. A. Hansen, L. Gundel, and T. Novakov, "Identification of the Optically Absorbing Component of Urban Aerosols," Applied Optics, vol. 17, 1978, p. 3859.

2. R. Weiss, R. J. Charlson, A. P. Waggoner, M. B. Baker, D. Covert, D. Thorsell, and S. Yeun, "Application of Directly Measured Aerosol Radiative Properties to Climate Models," Atmospheric Aerosols: Their Optical Properties and Effects; A Topical Meeting on Atmospheric Aerosols, National Aeronautics and Space Administration Report NASA CP-2004.

3. J. M. Waldram, "Measurement of the Photometric Properties of the Upper Atmosphere," Transactions of Illuminating Engineering Society London IU, 147, 1945.

4. C. I. Lin, M. B. Baker, and R. J. Charlson, "Absorption Coefficient of Atmospheric Aerosol: A Method of Measurement," Applied Optics, vol. 12, 1973, p. 6.

5. H. E. Gerber, "Absorption of 632.8 nm Radiation by Maritime Aerosols Near Europe," Journal of Atmospheric Sciences, vol. 36, 1979, p. 2502.

6. K. Fisher, "Mass Absorption Coefficient of Natural Aerosol Particles in the .4-2.4 μm Wavelength Interval, Beitr. zur Physik der Atmos. vol. 46, 1973, p. 89.

7. J. D. Lindberg, and L. S. Laude, "Measurement of the Absorption Coefficient of Atmospheric Dust," Applied Optics, vol. 13, 1974, p. 1923.

8. A. D. A. Hansen, H. Rosen, R. L. Dod, and T. Novakov, "Optical Characterization of Ambient and Source Particulates," Proceedings, Conference on Carbonaceous Particles in the Atmosphere. Lawrence Berkeley Laboratory report LBL-9037, p. 116.

9. H. Rosen, A. D. A. Hansen, R. L. Dod, and T. Novakov, "Soot in Urban Atmospheres: Determination by an Optical Absorption Technique," Science, vol. 208, 1980, p. 741.

10. F. R. Faxfog and D. M. Roessler, "Carbon Aerosol Visibility vs. Particle Size Distribution," Applied Optics, vol. 17, 1979, p. 2612.

11. D. M. Roessler and F. R. Faxfog, "Optical Properties of Agglomerated Acetylene Smoke Particles at .5145 μm and 10.6 μm Wavelength," Journal of Optical Society of America, vol. 70, 1980, p. 230.

12. T. Novakov, "Chemical Characterization of Atmospheric Pollution Particulates by Photoelectron Spectroscopy," Proceedings, Second Joint Conference on Sensing of Environmental Pollutants (Pittsburgh, Pa. Instrument Society of America, 1973), p. 197.

DETERMINATION OF BLACK CARBON BY THERMAL ANALYSIS*

L. Gundel, R. Dod, and T. Novakov

INTRODUCTION

Aerosol particulate material collected from ambient air and combustion sources always contains carbonaceous particles which are black or grey when collected on filters.[1] The absorption of visible light by these carbonaceous aerosols is predominantly due to the presence of carbon, which has optical properties similar to graphitic or elemental carbon and to activated carbon.[2,3] The term "black carbon" is used in this paper to refer to the optically absorbing carbonaceous component of ambient and source aerosols. Black carbon is implicated in visibility reduction,[4,5] and it could have effects on the tropospheric energy balance which could lead to regional and global climate modifications.[4,5]

Previous work at Lawrence Berkeley Laboratory (LBL) has shown that attenuation of visible light as it passes through ambient or source-particulate-loaded filters is related to concentrations of black carbon.[1,6] Attenuation measurements show that black carbon appears as a constant fraction of the total carbon contained in daily filter samples collected for two years at various urban sites throughout the United States.[6] Selective solvent extraction studies have shown that black carbon is nonextractable,[1] as expected for elemental carbon. In order to measure concentrations of black carbon on filters by optical attenuation, a direct determination of black carbon is necessary.

One method of identifying black carbon is optico-thermal analysis,[7] a combustion thermal analysis in which both the product CO_2 concentration and the optical transmission of the material are continuously monitored. This method yields simultaneous measurement of the amount of particulate carbon burned and of the change in light transmission through the filter sample as temperature-programmed combustion proceeds. For some types of samples, primarily those collected directly from combustion sources, the black carbon can be unambiguously identified and quantified from the thermogram, as shown in Figure 1a. Differentiation of black carbon from organic carbon in thermograms of ambient particulate samples may be more difficult, as illustrated in Figure 1b. Thermograms of ambient samples sometimes show carbonization, as indicated by a decrease in light transmission during thermal analysis. An example of this is shown in Figure 1c, where production of black carbon during analysis compounds the difficulty of isolating the original black carbon. Removal of soluble organic material by selective solvent extraction before thermal analysis leads to thermograms in which isolation of the black carbon peak is straightforward.[8]

ACCOMPLISHMENTS DURING FY 1980

Experimental Methods

Determination of black carbon in urban ambient and source particulate material has been accomplished by complementary use of optico-thermal analysis (as described above) and selective solvent extraction. The selective solvent extraction technique is based on the work of Appel et al.,[9,10] in which a filter sample is subjected to soxhlet extraction in benzene, followed by extraction in a methanol-chloroform mixture (1:2, v:v). This procedure removes most of the nonblack organic carbon but leaves the optical attenuation unchanged to within 10%. Optico-thermal analysis is performed on untreated particulate carbon samples and on portions of the same material after solvent extraction. For each extracted sample the amount of black carbon is determined by measuring the area under the CO_2 peak, which corresponds to the decrease in blackness, as shown by increased light transmission. Since the gas flow through the apparatus is constant, as is the temperature ramp, this area is proportional to the total mass of black carbon. Optical attenuation, ATN, is defined as

$$ATN = 100 \ln I_0/I, \qquad (1)$$

where I and I_0 represent the intensity of light transmitted through the filter before combustion and after removal of the black carbon by combustion, respectively. Optical attenuation values may depend on the type of filter substrate and on measurement technique.

Black Carbon in Ambient and Combustion Source Particulate Matter

Figure 2 shows thermograms of ambient particulate carbon collected near LBL and near the Eastshore Freeway in Berkeley, Calif. during the same 24-hour period. The patterns for the untreated samples are typical for urban particulate matter. The freeway particulate carbon thermogram shows enrichment in high temperature carbon. Total carbon and ATN are also higher for the freeway sample. After extraction, thermograms for both samples show a simpler structure. The black carbon peaks have been indicated by shading in the figure. Note that some nonblack carbon remains after extraction and that black carbon accounts for only part of the high temperature peak of the untreated sample collected at LBL (Fig. 2a).

*This work was supported by the Assistant Secretary for Environment, Office of Health and Environmental Research, Division of Biomedical and Environmental Research of the U.S. Department of Energy under Contract No. W-7405-ENG-48 and by the National Science Foundation under Contract No. ATM 80-13707.

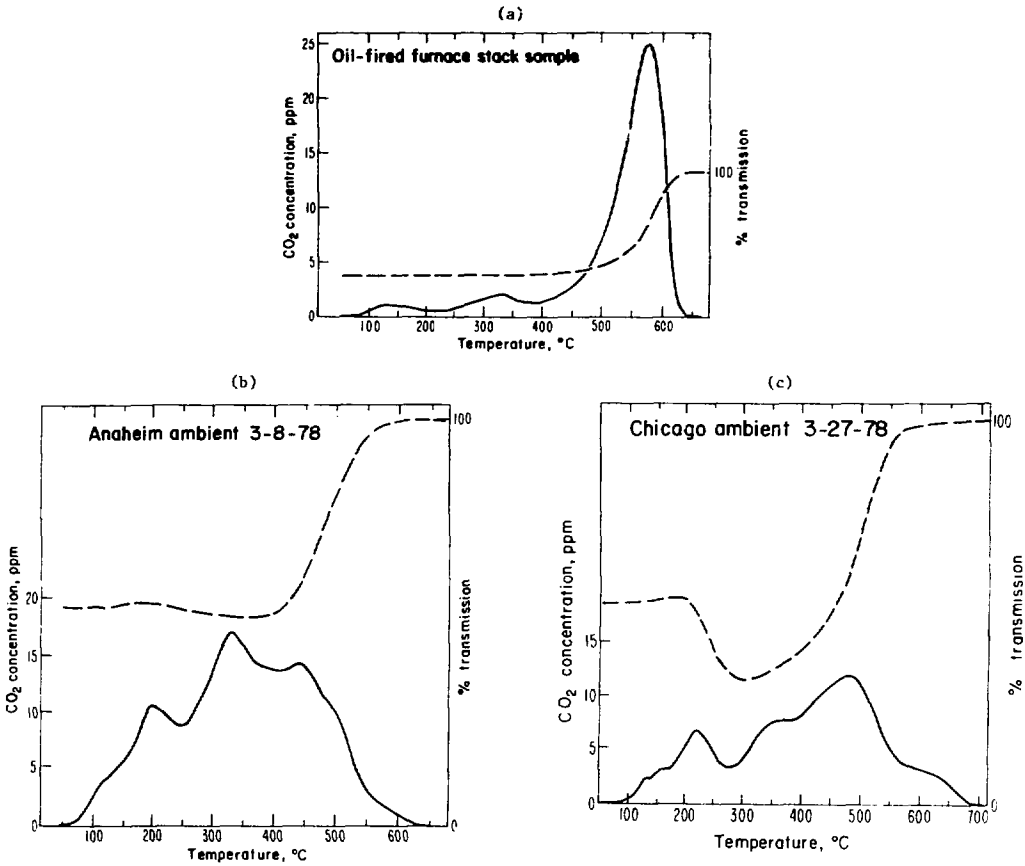

Fig. 1. Thermograms of particulate carbon collected from (a) oil-fired furnace; (b) Anaheim, Calif.; (c) Chicago, Ill. [(a) XBL 791-157; (b) XBL 791-159; (c) XBL 791-161]

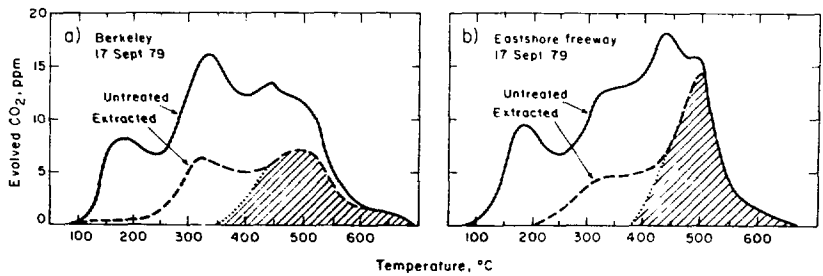

Fig. 2. Thermograms of particulate carbon collected in Berkeley, Calif. and near a major highway for untreated and sequentially extracted filter samples. The shaded area represents the black carbon. (XBL 811-40)

Thermograms for typical combustion sources are shown in Figure 3. Particulate carbon from the natural gas and propane samples is dominated by black carbon, as shown by comparison of their thermograms before and after extraction. Particulate carbon samples collected in a parking garage and in the Caldecott tunnel contain large amounts of organic as well as black carbon. Although the combustion characteristics of the black carbon in these source samples may be changed by extraction to produce temperature shifts, for example, the amount of carbon represented by the high temperature peak can be ascribed to black carbon in both extracted and unextracted samples.

The Relationship Between Optical Attenuation and Black Carbon Concentration

Figures 4 and 5 show the relationship between optical attenuation and concentration of black carbon for urban and combustion source particulate carbon respectively, as measured by optico-thermal analysis. In each case the line is a linear least squares fit to the data. The slopes of the fitted lines are 18.9 for ambient and 19.1 for source particulate matter, expressed in units of optical density/$\mu g\text{-}cm^{-2}$. Correlation coefficients are 0.98 and 0.99, respectively. Within experimental error, the slopes are identical. This indicates that the black carbon produced by these sources has the same optical properties as black carbon present in urban particulate matter. This agreement with the results of other work at LBL[2,6] supports the validity of measurement of concentrations of black carbon and ATN by optico-thermal analysis of preextracted filter samples.

The results presented here show that we now have a method for determination of the specific attenuation[2,6] σ of black carbon, where

$$\sigma = ATN/[C] \qquad (2)$$

σ has the value 19 optical density units/$\mu g\ cm^{-2}$ black carbon, when ATN and concentration of black carbon are measured by the method described here.

Planned Activities for FY 1981

We will determine the relationship between ATN as measured by this method and ATN as measured using the standard LBL technique.[1] We will participate in a study sponsored by General Motors Research Laboratories to compare methods used by various laboratories to measure black carbon concentrations in carbonaceous particulate matter.

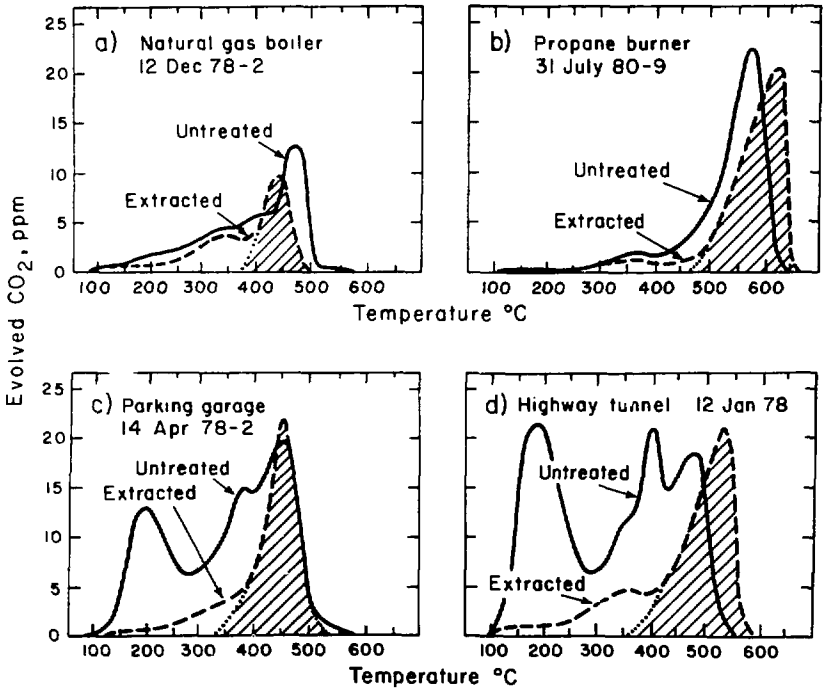

Fig. 3. Thermograms for combustion-source-generated particulate carbon for untreated and solvent extracted filter samples. The shaded area represents the black carbon. (XBL 811-39)

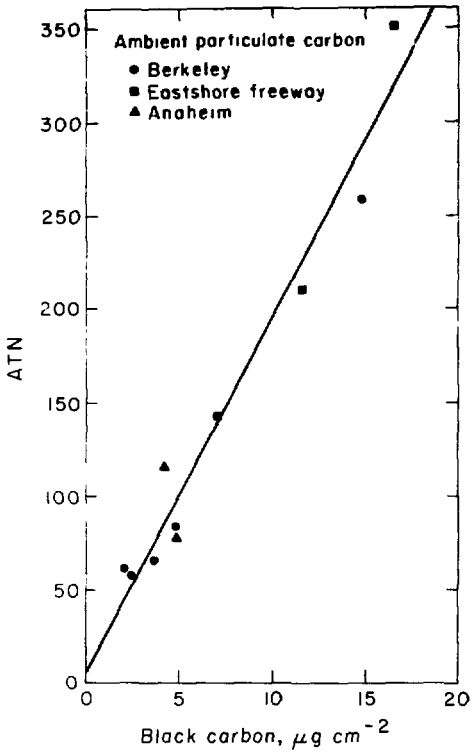

Fig. 4. Results of optico-thermal analysis for ambient particulate carbon: ATN versus amount of black carbon for samples collected in Berkeley (●), near a major highway (■), and in Anaheim, Calif. (▲). The amount of black carbon is determined from the area of the optically absorbing peak in the thermogram of the extracted filter sample. (XBL 811-37)

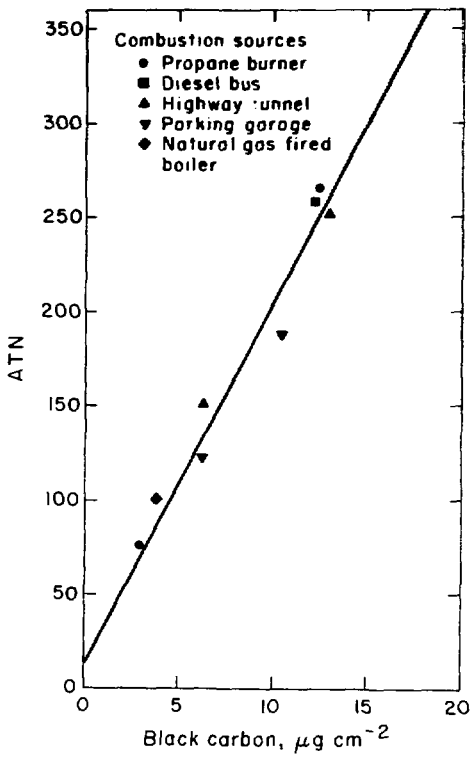

Fig. 5. Results of optico-thermal analysis for combustion-source generated particulate carbon: ATN versus amount of black carbon for a propane burner (●), a diesel bus, idling (■), a highway tunnel (▲), a parking garage (▼), and a natural gas fired boiler (◆). (XBL 811-38)

Further work is in progress to determine what particulate sample properties affect the combustion temperature of black carbon.

REFERENCES

1. H. Rosen, A. D. A. Hansen, L. Gundel, and T. Novakov, "Identification of the Optically Absorbing Component in Urban Aerosols," Applied Optics, vol. 17, 1978, p. 3859.

2. H. Rosen and T. Novakov, "Raman Scattering and the Characterization of Atmospheric Aerosol Particles," Nature, vol. 266, 1977, p. 708.

3. Z. Yasa, N. M. Amer, H. Rosen, and A. D. A. Hansen, "A Photoacoustic Investigation of Urban Aerosol Particles," Applied Optics, vol. 18, 1979, p. 2528.

4. R. E. Weiss, A. P. Waggoner, R. J. Charlson, D. L. Thorsell, J. S. Hall, and L. A. Riley, "Studies of the Optical, Physical, and Chemical Properties of Light Absorbing Aerosols," Proceedings, Conference on Carbonaceous Particles in the Atmosphere, Lawrence Berkeley Laboratory report LBL-9037, 1979.

5. H. Rosen, T. Novakov, and B. A. Bodhaine, Soot in the Arctic, Lawrence Berkeley Laboratory report LBL-11648, 1980.

6. A. D. A. Hansen et al., "The Use of an Optical Attenuation Technique to Estimate the Carbonaceous Component of Urban Aerosols," Atmospheric Aerosol Research FY 1979, Lawrence Berkeley Laboratory Report LBL-10735, 1980, p. 16.

7. R. L. Dod, H. Rosen, and T. Novakov, "Optico-Thermal Analysis of the Carbonaceous Fraction of Aerosol Particles," Atmospheric Aerosol Research Annual Report, 1977-78, Lawrence Berkeley Laboratory report LBL-8696, 1979, p. 2.

8. L. Gundel, R. Dod, and T. Novakov, "Application of Selective Solvent Extraction and Thermal Analysis to Ambient and Source Enriched Aerosols," Atmospheric Aerosol Research FY 1979, Lawrence Berkeley Laboratory report LBL-10735, 1980, p. 27.

9. B. R. Appel, E. M. Hoffer, E. L. Kochev, S. M. Wall, M. Haik, and R. L. Knights, "Analysis of Carbonaceous Material in Southern California Atmospheric Aerosols," Environmental Science and Technology, vol. 13, 1979, p. 98.

10. L. A. Gundel, G. E. Mason, and T. Novakov, "Characterization of Source and Ambient Particulate Samples by Solvent Extraction," Atmospheric Aerosol Research Annual Report, 1977-78, Lawrence Berkeley Laboratory report LBL-8696, 1979, p. 63.

A MODEL FOR THE PROGRESSIVE COMBUSTION ANALYSIS OF CARBONACEOUS AEROSOL PARTICLES*

A. Hansen and T. Novakov

INTRODUCTION

The analysis of aerosol particles by progressive thermal decomposition was first reported by Malissa et al.[1] and has subsequently been developed into a powerful method for the qualitative and quantitative analysis of carbonaceous and nitrogenous aerosols.[2,3] This paper presents a model for the combustion process that may be fit to the data to yield further information on the nature of the carbonaceous species.

ACCOMPLISHMENTS DURING FY 1980

The analytical method subjects the sample to a steadily increasing temperature in an atmosphere of pure oxygen. The evolved gas is passed over an oxidizing catalyst, and the CO_2 concentration is recorded. The technique is similar to that of the flash desorption spectrometer[4] used in studies of surface bonding. Most ambient samples yield complex traces of carbon evolution versus temperature due to the presence of many different classes of compounds. However, certain samples may be chosen or selectively pretreated so that the "thermogram" shows a single set of distinct characteristics, suggesting a process of combustion at elevated temperatures. Figure 1a shows this trace for a diesel exhaust sample; when displayed as an Arrhenius plot (Fig. 1b), it is clear that the trace is characteristic of a thermally activated process, with a slope corresponding to an activation energy of 26.9 kcal/mol. Other samples may show different slopes or maxima (see Fig. 1c for aerosol collected from an oil-fired furnace). The model has been designed to interpret these traces in terms of underlying physical and chemical characteristics.

Considering the combustion of a homogeneous single component material, we write the rate of reaction of a carbon atom exposed to oxygen at time t, temperature T(t) as

$$P(T) = C \cdot T^{\alpha} \cdot \exp(-E_a/T), \qquad (1)$$

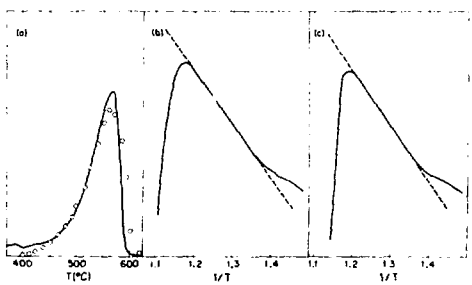

Fig. 1. Experimental data and fit: (a) Evolved CO_2 versus temperature for diesel exhaust particulate sample. Solid curve indicates experimental data; circles indicate best fit to Equation (3) with parameters E_a = 26.9 kcal/mol, rate constant $C = 6.0 \times 10^5$ sec^{-1}, and three-dimensional combustion geometry. (b) Arrhenius plot of Figure 1(a): $\log(CO_2)$ versus inverse temperature. Dashed line slope corresponds to activation energy of 26.9 kcal/mol. (c) Arrhenius plot of data from oil-fired furnace stack sample. Dashed line slope corresponds to activation energy of 25.9 kcal/mol. (XBL 811-7672)

*This work was supported by the Assistant Secretary for Environment, Office of Health and Environmental Research, Division of Biomedical and Environmental Research of the U. S. Department of Energy under Contract No. W-7405-ENG-48 and by the National Science Foundation under Contract No. ATM 80-13707.

where E_a is the activation energy (in degrees K), C is the rate constant, and the exponent α represents the temperature dependence of the rate of collision of oxygen molecules with the carbon atom. If there are n such atoms, all equally exposed, their rate of removal from the sample is

$$-\frac{dn}{dt} = nP(T). \qquad (2)$$

Since the temperature T is a function of time t, this equation does not have a simple analytic solution, and discrete-step numerical methods must be used.

Other work has shown that the carbon species responsible for high-temperature (~500°C) thermogram traces may be in the form of graphitic microcrystallites of dimension ~30Å.[5] This could result in the exclusion from combustion of the atoms interior to the reacting surfaces or plane edges. Equation (2) is then modified to become

$$-\frac{d}{dt}(\log n) = B\, n^{\beta}\, P(T), \qquad (3)$$

where the constant B depends on geometry and packing fraction, and the exponent β is zero if all atoms are exposed, (-1/2) for two-dimensional combustion from the edges of graphitic planes, or (-1/3) for combustion from the outer surface of a sphere.

The presence of carbon in i different forms will produce a net yield of

$$\frac{dN}{dt} = \sum_i \frac{dn_i}{dt}$$

if the components are noninteracting. However, for the case of internally mixed particles, it is plausible that the combustion of an atom j may increase the probability of combustion of a neighboring atom i--an effect similar to ignition. This is modelled by increasing the combustion probability of the atom i by $[P_i(T + \tau_{ij}) - P_i(T)]$ for each atom of component j that burns with probability $P_j(T)$. The fraction of these is (n_j/N) and so Equation (3) becomes

$$-\frac{d}{dt}(\log n_i) = BN^{\beta}\left\{P_i(T) + \sum_j (n_j/N)[P_i(T + \tau_{ij}) - P_i(T)]\cdot P_j(T)\right\} \qquad (4)$$

The matrix elements τ_{ij} represent the coupling of combustion energy among neighboring atoms; diagonal elements represent intraspecies self-ignition.

For single component combustion, the effect of τ_{11} is to sharpen the trace (Fig. 2a); for a two-component mixture the off-diagonal elements result in a reduction of the higher temperature peak (Fig. 2b). With simplifying assumptions,

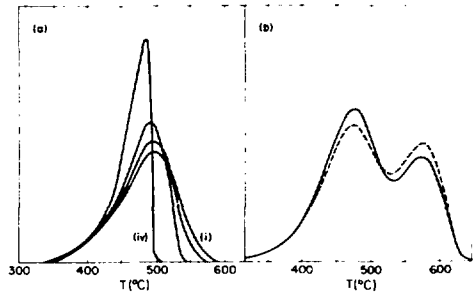

Fig. 2. Simulated curves calculated from Equation (4), illustrating intercomponent coupling. (a) Single component. Activation energy 28 kcal/mol, rate constant 2×10^6 sec^{-1}. Curves (i) - (iv) show the progression of coupling temperatures τ_{11} = 0, 100, 150, 200K. (b) Two components. Activation energies 27 and 31 kcal/mol, equal quantities, and equal rate constants 2×10^6 sec^{-1}. Dashed curve indicates no coupling. Solid curve indicates all τ_{ij} = 150K. (XBL 811-7673)

Equation (4) may be fit to experimental data to yield best values of the parameters.

In conclusion, we have shown that a progressive combustion model can account for experimental data from the analysis of carbonaceous aerosol particles and can yield reasonable parameters when fit to those data. We wish to thank Dr. R. Schefer of the Combustion Research Group (LBL) for helpful discussions.

PLANNED ACTIVITIES FOR FY 1981

Future work will be aimed at improving the fitting capability so that the full form of Equation (4) may be used to extract morphological and ignition-coupling information from experimental data.

REFERENCES

1. H. Malissa, H. Puxbaum, and E. Pell, "Zur Simultanen Relativkonduktometrischen Kohlenstoff und Schwefelbestimmung in Stäuben," Zeitschrift für Analytische Chemie, vol. 282, 1976, p. 109.

2. R. L. Dod, H. Rosen, and T. Novakov, "Optico-Thermal Analysis of the Carbonaceous Fraction of Aerosol Particles," Atmospheric Aerosol Research Annual Report, 1977-78, Lawrence Berkeley Laboratory report LBL-8696, 1978, p. 2.

3. R. L. Dod et al., "Application of Thermal Analysis to the Characterization of Nitrogenous Aerosol Species," Atmospheric Aerosol Research Report FY 1979, Lawrence Berkeley Laboratory report LBL-10735, 1980, p. 35.

4. H. D. Hagstrum, "Instrumentation and Experimental Procedure for Studies of Electron Ejection by Ions and Ionization by Electron Impact," Review of Scientific Instruments, vol. 24, 1953, p. 1122.

5. H. Rosen, A. D. A. Hansen, L. Gundel, and T. Novakov, "Identification of the Optically Absorbing Component in Urban Aerosols," Applied Optics, vol. 17, 1978, p. 3859.

RELATION BETWEEN CONCENTRATIONS OF POLYNUCLEAR AROMATIC HYDROCARBONS AND BLACK CARBON*

L. Gundel, H. Rosen, and T. Novakov

INTRODUCTION

We have developed an optical attenuation technique[1] to measure the black carbon content in particulate material. In addition to the black carbon, particulate organic carbon in ambient aerosols also contains primary organics, directly produced from combustion sources.[2] This primary organic carbon together with black carbon is defined as "soot." We have studied the relationship between the black carbon concentration and one class of primary organic compounds, polynuclear aromatic hydrocarbons (PAH) in urban carbonaceous particles. These compounds and their oxidized derivatives may constitute the health hazard associated with ambient and source carbonaceous particles.[3-5]

ACCOMPLISHMENTS DURING FY 1980

Experimental Methods

The samples used in this study were selected from loaded (47-mm diameter) quartz filters collected as part of the Lawrence Berkeley Laboratory sampling program during the summer of 1980.[6] Optical attenuation (ATN) measurements were made on Millipore cellulose acetate filters collected simultaneously. ATN is defined as equal to 100 ln I_0/I, where I_0 and I are the intensities of light transmitted through blank and loaded filters, respectively. ATN has units of optical density per 10^6 m air.

For determination of PAH concentrations on each filter sample, one section (1.94 cm^2) of the quartz filter was extracted in 0.400 ml peroxide-free spectral quality tetrahydrofuran by sonication at 25°C for 15 min.[7] A 50-µl aliquot of the extract was injected onto a liquid chromatographic column, which had been chosen for its selectivity for separation of PAH compounds[8] (VYDAC 201TP, 10-µm particle size, 25-cm length, 0.46 cm i.d.). The hydraulic system was purchased from Waters, Inc. A mixture of acetonitrile and tetrahydrofuran (19:1, v:v) in water was used as the mobile phase at a flow rate of 3.0 ml min^{-1}. Composition of the acetonitrile-tetrahydrofuran mixture varied from 70-98% in 30 min using Waters' gradient #9. The separated PAH compounds were detected with a Schoeffel Model SF970 fluorescence detector with excitation wavelength set at 280 nm. All fluorescence at wavelengths $\geq$ 389 nm was recorded as the sample eluted from the column. PAH standard compounds were supplied by Pfaltz and Bauer, Aldrich Chemical Co., and Nanogens, Inc. Peak heights were used for measurement of concentrations of PAH in the extracts of ambient particulate loaded filters.

Identification of PAH compounds from retention times of fluorescent peaks in chromatograms of ambient extracts was accomplished by comparison to retention times of PAH standards. The fluorescence ratio technique[9] was used to confirm the assignments. Identification by this technique requires that the ratios of peak intensities for several wavelength combinations of excitation, λ_{ex}, and emission, λ_{em}, match for an extract peak and a known PAH peak with the same retention time.

Results

Figure 1 shows chromatograms for a mixture of PAH compounds and for a typical filter extract. The major fluorescent compounds have been identified as benzo(b)fluoranthene, benzo(k)fluoranthene, benzo(a)pyrene, benzo(ghi)perylene, and indeno(1,2,3-cd)pyrene. Some PAH compounds which fluoresce weakly under the same conditions were not detected: chrysene, benzo(e)pyrene, perylene, and dibenz(a,h)anthracene. The PAH compounds found in this study have been detected in urban particulate matter collected in other cities and in particulate samples[11] from combustion sources.

Figure 2 shows concentrations of benzo(a)pyrene (BaP), indeno(1,2,3-cd)pyrene (IcdP), and benzo(ghi)perylene (BghiP) plotted versus optical attenuation, ATN. The lines are linear least squares fits for the data. The benzofluoranthenes, BbF and BkF, show similar trends. The concentrations of these PAHs correlated with ATN as indicated in Table 1. Degradation of these PAH compounds by processes such as photo-oxidation or

*This work was supported by the Assistant Secretary for Environment, Office of Health and Environmental Research, Division of Biomedical and Environmental Research of the U.S. Department of Energy under Contract No. W-7405-ENG-48 and by the National Science Foundation under Contract No. ATM 80-13707.

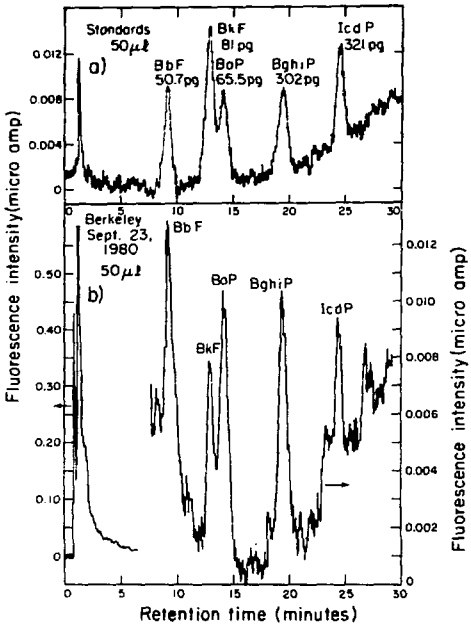

Fig. 1. Fluorescence chromatograms for (a) Mixture of PAH standard compounds. BbF = benzo(b)-fluoranthene; BkF = benzo(k)fluoranthene; BaP = benzo(a)pyrene; BghiP = benzo(ghi)perylene; IcdP = indeno(1,2,3-cd) pyrene; (b) Tetrahydrofuran extract of ambient carbonaceous particles. (XBL 8101-42)

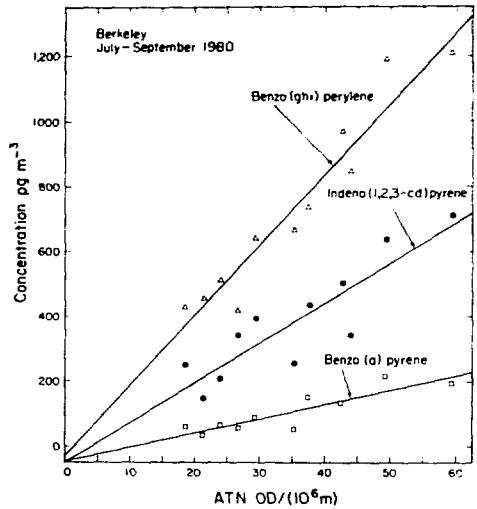

Fig. 2. The relationship between concentrations of three polynuclear aromatic hydrocarbons and optical attenuation ATN, a measure of black carbon concentration. (XBL 8101-41)

Table 1. PAH concentrations, total carbon, and attenuation data for carbonaceous particles collected in Berkeley, Calif., July-September 1980.

	Average [PAH]	[PAH] versus ATN		
	($pg\ m^{-3}$)	Slope	Intercept	r
Benzo(b)fluoranthene (BbF)	82 ± 29	1.76	20.0	0.76
Benzo(k)fluoranthene (BkF)	82 ± [illegible]	1.66	23.0	0.76
Benzo(a)pyrene (BaP)	106 ± 6[illegible]	3.82	-34.2	0.75
Benzo(ghi)perylene (BghiP)	730 ± 290	21.8	-35.1	0.96
Indeno(1,2,3-cd)pyrene (IcdP)	380 ± 180	12.3	-48.6	0.88
		[C] versus ATN		
	Average Values	Slope	Intercept	r
Total carbon ($\mu g\ m^{-3}$)	7.3 ± 2.1	5.64	-7.30	0.93
ATN (o.d. $10^{-6}\ m^{-1}$)	35 ± 13	--	--	--

reaction with pollutant gases[12] may account for some of the scatter observed. BghiP shows the largest correlation coefficient (r = 0.96) and BaP, the smallest (r = 0.75). These values are consistent with the observation that BghiP is less susceptible to degradation than is BaP.[13] The average correlation coefficient relating [PAH] to total carbon (r = 0.78) is close to the average correlation coefficient relating [PAH] to ATN (r = 0.82).

Conclusion

The preliminary results presented here establish a linear relationship between concentration of several polynuclear aromatic hydrocarbons and optical attenuation as measured on filter samples of carbonaceous particles collected in Berkeley, Calif., during the summer of 1980. Since ATN measures the amount of black carbon, our results show that concentrations of PAH's are proportional to black carbon concentrations. Measurement of ATN may provide a fast and simple method to estimate concentrations of PAH compounds in particulate matter collected in Berkeley.

The authors thank A. Hansen for providing optical attenuation and total carbon concentration data.

PLANNED ACTIVITIES FOR FY 1981

Future work is to include measurement of PAH concentrations and ATN for carbonaceous particles collected in other cities that are part of the LBL sampling network. Concentrations of oxidized derivatives of PAH compounds will be measured to determine what relationship may exist between their concentrations and the blackness of urban carbonaceous particles.

REFERENCES

1. H. Rosen, A. D. A. Hansen, L. Gundel, and T. Novakov, "Identification of the Optically Absorbing Component in Urban Aerosols," Applied Optics, vol. 17, 1978, p. 3859.

2. D. Schuetzle, D. Cronn, A. L. Crittenden, and R. J. Charlson, "Molecular Composition of Secondary Aerosol and its Possible Origin," Environmental Science and Technology, vol. 9, 1975, p. 838.

3. Y. Y. Wang, S. M. Rappoport, R. F. Sawyer, R. E. Talcott and E. Wei, "Direct Acting Mutagens in Automobile Exhaust," Cancer Letters, vol. 5, 1978, no. 39.

4. J. N. Pitts, Jr., D. Grosjean, and T. Mischke, "Mutagenic Activity of Airborne Particulate Organic Pollutants," Toxicology Letters, vol. 1, 1977, p. 65.

5. D. Schuetzle, F. S-C. Lee, T. J. Prateer, and S. B. Tejada, "The Identification of Poly-Nuclear Aromatic Hydrocarbon Derivatives in Mutagenic Fractions of Diesel Particulate Extracts," International Journal of Environmental and Analytical Chemistry, (in press).

6. A. D. A. Hansen et al., "The Use of an Optical Attenuation Technique to Estimate the Carbonaceous Component of Urban Aerosols," Atmospheric Aerosol Research FY 1979, Lawrence Berkeley Laboratory report LBL-10735, 1980, p. 16.

7. C. Golden and E. Sawicki, "Ultrasonic Extraction of Total Particulate Aromatic Hydrocarbons (TpAh) From Airborne Particles at Room Temperature," International Journal of Environmental and Analytical Chemistry, vol. 4, 1975, p. 9.

8. K. Ogan and E. Katz, "Retention Characteristics of Several Bonded-Phase Liquid Chromatography Columns for some Polycyclic Aromatic Hydrocarbons," Journal of Chromatography, vol. 188, 1980, p. 115.

9. B. S. Das and G. H. Thomas, "Fluorescence Detection in HPLC Determinations of Polycyclic Aromatic Hydrocarbons," Analytical Chemistry, vol. 50, 1978, p. 967.

10. For a summary, see Ontario Ministry of the Environment, Polynuclear Aromatic Hydrocarbons, Air Resources Branch, ARB-TDA Report Number 57-79, 1979, p. 146.

11. J. M. Daisey, M. A. Leyko, and T. J. Kneip, "Source Identification and Allocation of Polynuclear Aromatic Hydrocarbon Compounds in the New York City Aerosol," Polynuclear Aromatic Hydrocarbons, P. W. Jones and P. Lever (Ann Arbor, Mich.: Ann Arbor Science, 1979), p. 201.

12. J. N. Pitts, Jr., K. A. Van Cauwenberghe, D. Grosjean, J. P. Schmid, D. R. Fitz, W. L. Belser, G. B. Knudson, P. M. Hynds, "Atmospheric Reactions f Polycyclic Aromatic Hydrocarbons: Facile Formation of Mutagenic Nitro Derivatives," Science, vol. 202, 1978, p. 515.

13. M. N. Iscoe, "Photochemical Changes in Thin Layer Chromatograms of Polycyclic Aromatic Hydrocarbons," Analytical Chemistry, vol. 36, 1964, p. 2505.

DETERMINATION OF CARBON IN ATMOSPHERIC AEROSOLS BY DEUTERON-INDUCED NUCLEAR REACTIONS*

M. Clemenson, T. Novakov, and S. Markowitz

INTRODUCTION

Nuclear reactions induced by 7.6-MeV deuterons are used to determine total carbon in atmospheric aerosols. The $^{12}C(d,n)^{13}N$ reaction produced the radionuclide ^{13}N, a 10.0-min positron emitter which is detected by its 0.511-MeV annihilation radiation. The detection system is a Ge(Li) γ-ray spectrometer. The method is nondestructive of the sample, permitting the sample to be studied by additional methods. Comparison of carbon found by deuteron activation analysis with that found by independent but destructive combustion methods shows a standard deviation of 10% for 15 samples analyzed over a wide range of carbon contents. The detection limit is estimated to be 0.5 μg/cm^2, corresponding to a carbon concentration of 0.2% in a sample of total thickness 250 μg/cm^2.

ACCOMPLISHMENTS DURING FY 1980

Carbon has been found to be a major elemental constituent of urban particulate pollution.[1,2] The determination of the carbon's origin in terms of primary and secondary components is a difficult problem, to which a solution is necessary if meaningful control strategies are to be implemented. Some work has been done, but much more work is required.[3-5] Of important analytical concern is the nondestructive determination of the total carbon content of atmospheric aerosol samples. The common method of carbon determination in atmospheric aerosol samples is by combustion analysis. This method, however, is destructive of the sample, and thus does not allow other analyses to be performed on the same sample. A new method for the nondestructive determination of carbon and other low-Z elements in atmospheric aerosols has been developed by Macias and coworkers.[6] Their method involves the in-beam measurement of γ rays from the inelastic scattering of 7-MeV protons accelerated in a cyclotron. This type of analysis, however, does require lengthy use of accelerator time. Another method for the nondestructive determination of carbon has been developed by Gordon and coworkers.[7] This involves the measurement of prompt γ rays following neutron capture by using an external beam port of the National Bureau of Standards (NBS) research reactor as the neutron source. Relatively large samples (~1 g), however, and long irradiation periods (~20 hr) are required. A new activation-analysis method that uses only a short amount (2 min) of beam time for the determination of carbon in atmospheric aerosols will be described here. This method has already been used to determine nitrogen in aerosols, and future work will center on the development of a method for the determination of oxygen in aerosols.[8] General principles of charged-particle activation have been given by Markowitz and Mahony.[9]

The absolute excitation function for the $^{12}C(d,n)^{13}N$ reaction is shown in Figure 1. A comparison of results from the destructive combustion method with our deuteron activation method is given in Table 1. The ratio of "activation" to "combustion" carbon found averages 1.01 with a standard deviation of ±10%. A typical aerosol γ-ray spectrum is given in Figure 2. The decay of the 10-min ^{13}N activity is displayed in Figure 3.

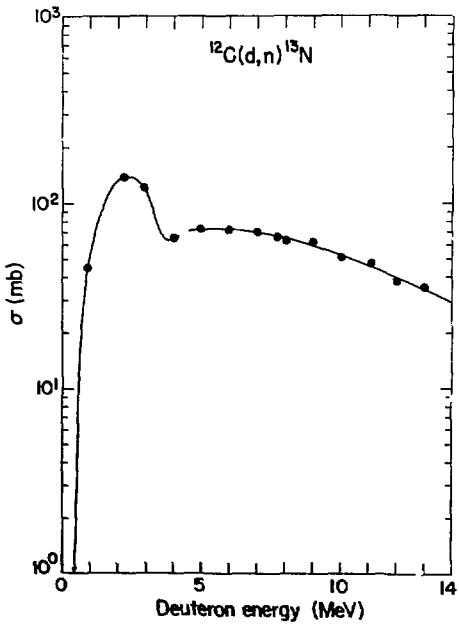

Fig. 1. Excitation function for the $^{12}C(d,n)^{13}N$ reaction. (XBL 797-2331)

*This work was supported by the Assistant Secretary for Environment, Office of Health and Environmental Research, Division of Biomedical and Environmental Research of the U.S. Department of Energy under Contract No. W-7405-ENG-48 and by the National Science Foundation under Contract No. ATM 80-13707.

Table 1. Comparison of methods for carbon determination in atmospheric aerosols.

Sample	Material	C Found ($\mu g/cm^2$) Deuteron Activation	C Found ($\mu g/cm^2$) Combustion	Ratio Activation/ Combination
AO-1	ammonium oxalate	218	210	1.04
AO-2	ammonium oxalate	268	224	1.20
AO-3	ammonium oxalate	131	122	1.07
AO-4	ammonium oxalate	74	62	1.19
AO-5	ammonium oxalate	109	113	0.96
AA-1	aerosol	84	85	0.99
AA-2	aerosol	100	99	1.01
AA-3	aerosol	106	111	0.95
AA-4	aerosol	76	76	1.00
AA-5	aerosol	103	100	1.03
AA-6	aerosol	93	93	1.00
AA-7	aerosol	5.2	4.8	1.08
AA-8	aerosol	0.6	0.7	0.86
AA-9	aerosol	57	62	0.92
AA-10	aerosol	28	32	0.88
				$\bar{R}$ = 1.01 ± 0.10

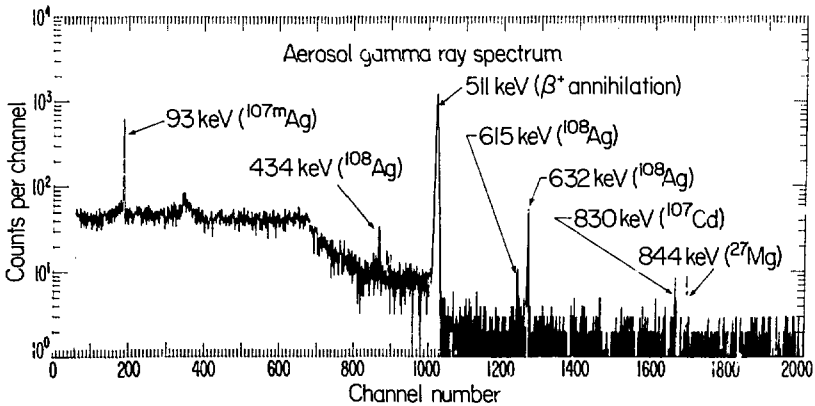

Fig. 2. The region from 0 to 1 MeV in the gamma ray spectrum of an aerosol sample following deuteron irradiation. (XBL 797-2335)

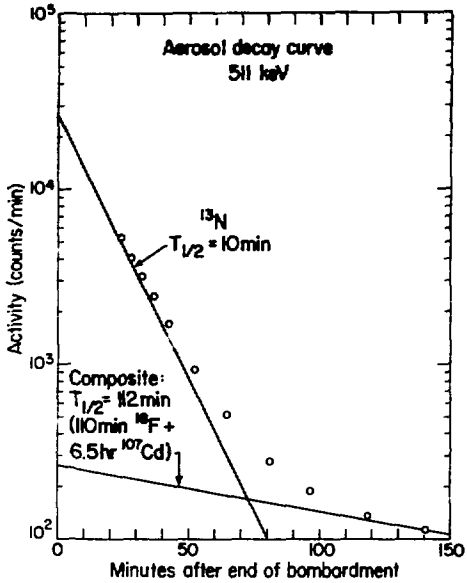

Fig. 3. Decay of the 0.511-MeV annihilation radiation activity following deuteron irradiation of an atmospheric aerosol sample. (XBL 797-2332)

PLANNED ACTIVITIES FOR FY 1981

Nuclear reaction work for the chemical analysis of atmospheric aerosols will continue.

REFERENCES

1. H. Malissa, "Some Analytical Approaches to the Chemical Characterization of Carbonaceous Particulates," Proceedings, Conference on Carbonaceous Particles in the Atmosphere, Lawrence Berkeley Laboratory report LBL-9037, 1979, p. 3.

2. Atmospheric Aerosol Research Annual Report, 1977-78, Lawrence Berkeley Laboratory report LBL-8696, 1978.

3. D. Grosjean, "Secondary Organic Aerosols and Mechanisms of Formation," Proceedings, Conference on Carbonaceous Particles in the Atmosphere, Lawrence Berkeley Laboratory report LBL-9037, 1979, p. 107.

4. R. L. Dod, H. Rosen, and T. Novakov, "Optico-Thermal Analysis of the Carbonaceous Fraction of Aerosol Particles," Atmospheric Aerosol Research Annual Report, 1977-78, Lawrence Berkeley Laboratory report LBL-8696, 1978, p. 2.

5. H. Rosen and T. Novakov, "Raman Scattering and the Characterization of Atmospheric Aerosol Particles," Nature, vol. 266, 1977, p. 708.

6. E. S. Macias, C. D. Radcliffe, C. W. Lewis, and C. R. Sawicki, "Proton Induced Gamma-Ray Analysis of Atmospheric Aerosols for Carbon, Nitrogen, and Sulfur Composition," Analytical Chemistry, vol. 50, 1978, p. 1120.

7. M. P. Failey, D. L. Anderson, W. H. Zoller, G. E. Gordon, and R. M. Lindstrom, "Neutron Capture Prompt Gamma-Ray Activation Analysis for Multielement Determination in Complex Samples," Analytical Chemistry, vol. 51, 1979, p. 2209.

8. M. Clemenson, T. Novakov, and S. S. Markowitz, "Determination of Nitrogen in Atmospheric Aerosols by Proton Activation Analysis," Analytical Chemistry, vol. 51, 1979, p. 572.

9. S. S. Markowitz and J. D. Mahony, "Activation Analysis for Oxygen and other Elements by Helium-3 Induced Nuclear Reactions," Analytical Chemistry, vol. 34, 1962, p. 329.

DETERMINATION OF LOW-Z ELEMENTS SIMULTANEOUSLY BY ^{3}HE-INDUCED NUCLEAR WASTES*

M. McKinney and S. Markowitz

INTRODUCTION

This work is a continuation of the work of Clemenson et al.[1,2] for developing rapid nondestructive techniques for determining carbon, nitrogen, and oxygen in atmospheric aerosols. X-ray fluorescence or neutron activation analysis can then be used to determine nearly all the higher Z elements. Combustion analysis could be used for these elements, but it is not sufficiently sensitive and the sample is destroyed.

Nondestructive techniques have been developed for determining these elements by Macias et al.,[3] Failey et al.,[4] and Gladney et al.;[5] these methods, however, require lengthy use of accelerator or reactor time and the latter method requires large samples. Previously Clemenson et al.[1,2] developed methods of determining carbon, nitrogen, and oxygen separately by activation analysis using different charged particles in different experiments. We want to develop a method for simultaneously determining carbon, nitrogen, and oxygen in atmospheric aerosols by irradiating the sample with a single particle.

ACCOMPLISHMENTS DURING FY 1980

The experiments are carried out using the stacked-foil technique. The standards and samples are irradiated with 20-MeV ^{3}He particles; the energy of the beam is degraded by placing aluminum foils of the desired thickness before the standard and between the standard and sample. The range-energy tables of Williamson, Boujot, and Picard[6] are used to calculate the required thickness. Mylar, a known polyester, is the standard.

The samples were irradiated for 0.5 min at 0.5 μA beam intensity; they were analyzed by detecting the 511-keV positron annihilation radiation using an Ortec Ge(Li) detector coupled to a Canberra Multichannel analyzer and printer. After 10 min, the decay curve is dominated by the $^{12}C(^3He,^4He)^{11}C$ and $^{16}O(^3He,p)^{18}F$ reaction products with half-lives of 20.4 min and 110 min respectively. By analysis of the decay curve using the CLSQ computer code,[7] we can determine the contributions to the activity from carbon and oxygen. The amounts of carbon and oxygen present were determined by the "relative" method of activation analysis. The end-of-bombardment activities of carbon and oxygen in the aerosol samples were compared with the activities from the known amounts of carbon and oxygen in the ~.0005-in. Mylar standard, from which the amounts of carbon and oxygen can be calculated. A typical decay curve of the sample is shown in Figure 1.

The aerosols were collected on a silver membrane filter in parallel with a quartz filter with the use of a vacuum pump. The aerosols collected on the quartz filters were analyzed using the combustion technique. Knowing the relative flow rates through the two filters permits us to compare the amounts of carbon in atmospheric aerosols determined by these techniques (see Table 1). No other satisfactory method exists for determining these small amounts of oxygen. Untreated silver filters give a blank value of 5 μg/cm^2 of carbon. With 8-10 MeV ^{3}He particles, no other interfering reactions are observed on the silver or aluminum; and the spectrum consists only of the 511-keV annihilation radiation and its Compton background.

PLANNED ACTIVITIES FOR FY 1981

In future experiments, we propose to make use of the $^{14}N(^3He, d)^{15}O$ reaction to simultaneously analyze for the nitrogen. The ^{15}O has only a 2-min. half-life, so it will be necessary to develop rapid methods of dismantling, mounting, and counting the samples at the 88-in. cyclotron instead of in our counting room.

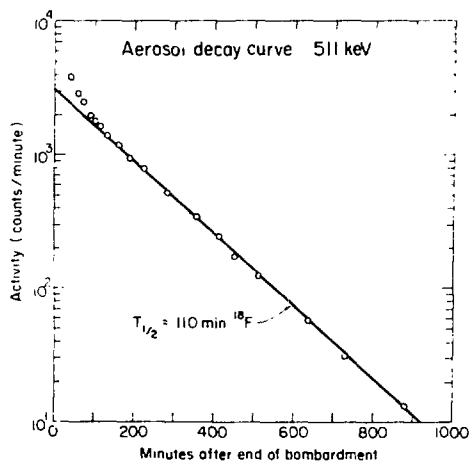

Fig. 1. Decay of the 0.511-MeV annihilation radiation following ^{3}He irradiation of an atmospheric aerosol sample. (XBL 7910-4325)

*This work was supported by the Assistant Secretary for Environment, Office of Health and Environmental Research, Division of Biomedical and Environmental Research of the U.S. Department of Energy under Contract No. W-7405-ENG-48 and by the National Science Foundation under Contract No. ATM 80-13707.

Table 1. Comparison of Carbon Analyses in Aerosols.

Aerosol	Combustion ($\mu g/cm^2$)	^3He activation ($\mu g/cm^2$)
1	30.6	27
2	12.0	14
3	40.0	39
4	50.0	54
5	56.0	40

REFERENCES

1. M. Clemenson, T. Novakov, and S. S. Markowitz, "Determination of Nitrogen in Atmospheric Aerosols by Proton Activation Analysis," Analytical Chemistry, vol. 51, 1979, p. 572.

2. M. Clemenson, T. Novakov, and S. S. Markowitz, "Determination of Carbon in Atmospheric Aerosols by Deuteron Activation Analysis," Analytical Chemistry, vol. 52, 1980, p. 175[illegible].

3. E. S. Macias, C. D. Radcliffe, C. W. Lewis, and G. R. Sawicki, "Proton Induced γ-ray Analysis of Atmospheric Aerosols for Carbon, Nitrogen, and Sulfur Composition," Analytical Chemistry, vol. 50, 1978, p. 1120.

4. M. P. Failey, D. L. Anderson, W. H. Zoller, G. E. Gordon, and R. M. Lindstrom, "Neutron Capture Prompt γ-ray Activation Analysis for Multielement Determination in Complex Samples," Analytical Chemistry, vol. 51, 1979, p. 1209.

5. E. S. Gladney, D. B. Curtis, and E. Jurney, "Simultaneous Determination of Nitrogen, Carbon, and Hydrogen by Thermal Neutron Prompt γ-ray Spectrometry," Analytical Chimica Acta, vol. 110, 1979, p. 339.

6. L. F. Williamson, J. P. Boujot, and J. Picard, "Tables of Range and Stopping Power of Chemical Elements for Changed Particles," J. Centre d'Etudes Nucleaires de Saclay Rapport CEA-R 3042, Paris, Documentation Francaise 1966.

7. J. B. Cumming, Applicacions of Computers to Nuclear and Radiochemistry, N.A.S.-N.R.C. Pub. NAS-NS 3107, 1963.

MEMBRANE BIOENERGETICS RESEARCH

MEMBRANE OXIDATIVE DAMAGE*

L. Packer, A. Quintanilha, R. Mehlhorn, O. Augusto, J. Maguire, and K. Davies

INTRODUCTION

Our studies have focused on the effects of environmental factors and pollution on mammalian cellular membranes. Our previous report[1-3] showed how sensitive to oxygen are isolated mitochondria, whole cells (hepatocytes and bacteria), model membranes, and enzymes.

Our working hypothesis has been that reactive species of oxygen, sometimes generated by endogenous cellular photosensitizers (flavins and hemes) in the presence of visible light, would react with cellular components thereby altering their structure and function. We have extended our work to studies of microsomal enzymes, particularly the very important drug metabolizing components NADPH-cytochrome-P_{450}-reductase and cytochrome P_{450}. The differential photosensitivity of the microsomal enzymes and the anaerobic component of the photoinactivation of NADPH reductase have enabled us to clarify different mechanisms of photodamage.

The use of a variety of different spin probes and their photomediated reduction and/or destruction has been a powerful tool in implicating free-radical intermediates in the mechanisms of photooxidative damage to biological membranes.

Free iron has been evaluated for its prooxidant effects; even at very low concentrations (μM), we have found that it will promote the auto-oxidation of epinephrine (a neural transmitter) and the formation of hydroxyl radicals ($OH^{\bullet}$) via the Fenton reaction.[2]

ACCOMPLISHMENTS DURING FY 1980

Microsomal Studies

We have been particularly interested in the mechanisms of initiation and of cellular damage by visible light (λ > 400 nm) through endogenous chromophores, in particular flavin coenzymes,[4-6] and the propagation of this damage by oxygen radicals.

The electron transport system in microsomes plays a vital role in xenobiotic metabolism, fatty acid desaturation and carcinogenesis, and contains both heme and flavin chromophores. The effect of visible light on microsomal electron transport components is shown[7] in Figure 1. There is a preferential inactivation of the NADPH-cytochrome-P_{450}-reductase and cytochrome P_{450}. In addition to protein inactivation, visible light also induces lipid peroxidation. Externally added flavin (FMN) increases both cytochrome P_{450} inactivation and lipid peroxidation. It is interesting that the reductase inactivation is not strictly oxygen-dependent since, to fully protect the enzyme, both anaerobiosis and a photoreductant, ethylene diamine tetra-acetic acid (EDTA) are required. The NADPH-reductase contains the photosensitive flavin cofactors, FMN and FAD. Following inactivation under anaerobic conditions, we have found that the NADPH-reductase can be largely reactivated by addition of FMN (but not FAD) suggesting that inactivation may be due to photomediated loss of FMN.

On the other hand, cytochrome P_{450} destruction appears to depend only on lipid peroxidation: Both processes are oxygen dependent, and are inhibited approximately to the same extent by antioxidants and radical scavengers. After FMN is lost and the NADPH-reductase is inactivated during anaerobic photosensitization, and the preparation

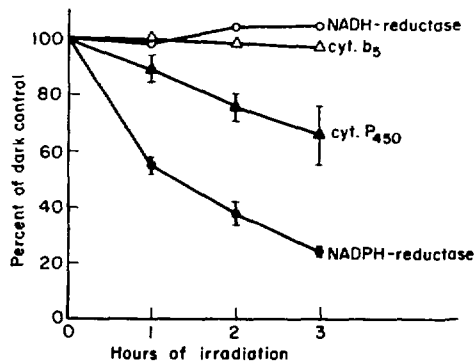

Fig. 1. Effect of visible light on microsomal electron transport activities. Data points are the average of results obtained with microsomes from two different rats; for clarity, the deviations are not shown for cytochrome b_5 and NADH-cytochrome b_5 reductase. Initial activities for the two preparations were: NADPH-cytochrome P_{450} reductase 100 and 96 nmol/min/mg; NADH-cytochrome b_5 reductase 1.7 and 3.0 μmol/min/mg, cytochrome P_{450} 0.8 and 0.7 nmol/min/mg;cytochrome b_5 0.5 and 0.4 nmol/mg. (XBL 806-3442)

*This work was supported by the Assistant Secretary for Environment, Office of Health and Environmental Research, Division of Life Sciences of the U.S. Department of Energy under Contract No. W-7405-ENG-48.

is further illuminated in the presence of air, we found that the extent of lipid peroxidation and cytochrome P_{450} destruction is a function of the NADPH-reductase activity left in the preparation. This suggests that lipid peroxidation and cytochrome P_{450} destruction are induced by the light excited flavin (FMN?) of the NADPH-reductase.

The greater photochemical reactivity of FMN as compared to FAD[8] could explain both the preferential inactivation of NADPH-reductase (NADH-reductase contains only FAD) as well as the selective destruction of FMN during illumination. Since it is known that cytochrome P_{450} reacts and is destroyed by hydroperoxides, whereas cytochrome b_5 is unaffected,[9] this may explain the differential inactivation of the microsomal cytochromes by visible light/O_2.

Photosensitized Nitroxide Spin Loss

Changes in the electron spin resonance (ESR) signal of nitroxide-free radicals were used to monitor very rapid light-induced free-radical reactions in inner mitochondrial membrane preparations.[10] After preincubation in the dark at 37°C for 2 h, illumination (at $\lambda > 400$ nm) of membranes in the presence of nitroxide probes (Fig. 2) showed that (a) oxidized probes are reduced and destroyed, and (b) reduced probes are oxidized and destroyed. The action spectrum of spin loss was shown to be similar to the absorption spectrum of FMN and was stimulated by the addition of exogenous flavin. However, in an aerobic model system containing buffer, FMN and oxidized nitroxide illumination has no effect on the ESR signal of the probe, whereas the reduced nitroxide is rapidly oxidized. Centrifugation experiments showed that flavines were released from the membrane during incubation

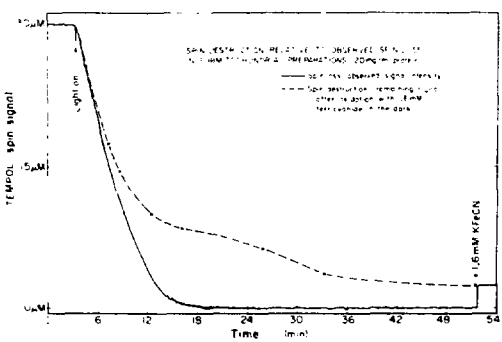

Fig. 2. Light dependent destruction, reduction and oxidation of TEMPOL and TOLH. 2 ml of SMP's were illuminated in 25 ml flasks in air and aliquots were withdrawn at the indicated times and examined either directly by ESR (spin loss) or after 2 min. of treatment with 1.6 mM of potassium ferricyanide (spin destruction). Buffer: 30 mM potassium phosphate, pH 7.4. Light intensity: 41 mW/cm^2. SMP's were preincubated in the dark at 37° C for 2 h. (XBL 773-3219)

and that the light-induced free radicals were generated in the aqueous environment of the membranes.

An interesting finding was that in the presence of 10 μM exogenous FMN, light causes the mitochondrial membrane to consume oxygen, suggesting the production of lipid peroxides. Positively charged spin probes exhibit considerably smaller light-induced spin-loss rates than either uncharged or negatively charged probes. An amphiphilic positively charged spin probe (CAT_{10}) was used to demonstrate that there is an irreversible rapid increase in negative surface charge[11] of the membranes during illumination.

Our experiments with exogenous flavins show the existence of a dark activation phenomenon other than flavin release. A "factor" is released from the membranes which may serve as the primary cofactor for spin destruction. The identification of this "factor", which is obviously important in free radical production and membrane damage, is presently under study.

Pro-oxidant Effects of Iron

Hydroxyl radical (OH•) production via the Fenton reaction[2] and epinephrine auto-oxidation can be propagated by catalytic amounts of iron. The role of iron in *in vivo* oxidative damage is of great relevance in many hydroxyl-radical investigations. In human iron toxicity studies, marked intracellular increases in the accumulation of hemosiderin and a lipofuscin-like pigment were observed[12], indicating an increase in the complex processes of damage that occur in the cell.

We have followed the rate of OH• generation via the Fenton reaction using bound iron as a catalyst.[13] The radical was trapped by 5,5' dimethyl-1-pyrroline-N-oxide (DMPO). Figure 3 shows that 10 μM Fe added as Fe^{+3}-EDTA gave rise to a substantial DMPO•OH signal. Even at 0.5 μM, iron was still effective. Ferritin (the chief form of storage of iron *in vivo*), even at a concentration equivalent to 100 μM, Fe did not give any signal; Transferrin (which serves as the main avenue of iron transport in the serum), with a bound iron concentration of 50 μM, also did not give any detectable signal. These results suggest that neither Ferritin nor Transferrin are able to propagate the Fenton reaction.

Epinephrine auto-oxidizes to adrenochrome rapidly at pH 10. Trace amounts of Fe^{+3}-EDTA were found to substantially increase the rate of auto-oxidation. However, neither Ferritin nor Transferrin had any effect on these rates. These results suggest that there are great differences in the catalytic capacity of iron when it is physiologically bound to proteins as compared to when it is chelated to EDTA (or DTPA, diethylene triamine penta-acetic acid).

PLANNED ACTIVITIES FOR FY 1981

Airborne pollutants generated by energy-related technologies pose a risk to human health. During exercise, pulmonary ventilation in animals and man increases exponentially in response to workload,

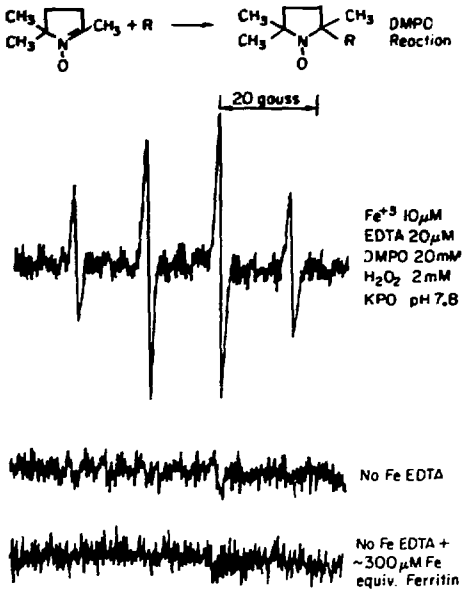

Fig. 3. Comparison of DMPO-OH signals by the reaction of differently bound forms of Fe and H_2O_2. (XBL 811-3586)

and the upper respiratory tract becomes less effective in removing pollutants.

In vivo tests will be made to measure the metabolic responses to exercise in man and small animals; the results will be correlated with biochemical and biophysical studies of whole organs, cells and subcellular parameters of animals. In vitro studies of lipid peroxidation will be correlated with in vivo activity through respiratory pentane production at rest and during exercise. The effects of different dietary levels of the anti-oxidant vitamin E will be investigated. Calorimetric systems will be used to monitor the effects of high ambient oxygen, argon, carbon monoxide, SO_2 and NO_x concentrations (and mixtures) on work capacity, endurance, oxygen consumption, and pentane production. Acute and chronic effects of exposure to these gases will be evaluated.

Our approach will lead to investigations of both basic research and applied research questions at the whole-animal level. Selected results will be verified with human subjects using noninvasive techniques. These studies will have special significance in the areas of membrane bioenergetics, exercise biochemistry, muscle and respiratory physiology, and environmental medicine.

REFERENCES

1. L. Packer, R. J. Mehlhorn, A. T. Quintanilha, B. Aggarwal, and J. J. Maguire, "Visible Light and Ozone Damage to Mammalian Membranes," Energy & Environment Division Annual Report 1977, Lawrence Berkeley Laboratory report LBL-6877, 1977, pp. 142-1[illegible].

2. L. Packer, A. T. Quintanilha, R. J. Mehlhorn, E. W. Kellogg, III, and J. J. Maguire, "Visible Light and Ozone Damage to Mammalian Cells and Membranes," Energy & Environment Division Annual Report 1978, Lawrence Berkeley Laboratory report LBL-8619, 1978, pp. 166-170.

3. L. Packer, A. Quintanilha, E. Kellogg, III, R. J. Mehlhorn, M. Nova, L. Cheng, and J. Maguire, "Membrane Oxidative Damage," Lawrence Berkeley Laboratory report LBL-11650, Energy and Environment Division Annual Report 1979, October 1980, pp. 7-5-7-7.

4. B. B. Aggarwal, A. T. Quintanilha, R. Cammack and L. Packer, "Damage to Mitochondrial Electron Transport and Energy Coupling by Visible Light", Biochimica et Biophysica Acta, vol. 502, no. 367, 1978.

5. L. Y. L. Cheng and L. Packer, "Photodamage to Hepatocytes by Visible Light" FEBS Letters, vol. 97, 1979. pp. 124-128.

6. L. Packer and E. W. Kellogg III, "Photooxidative Damage to Mammalian Cells and Proteins by Visible Light" American Chemical Society Symposium, vol. 123, 1980, pp. 83-93.

7. O. Augusto and L. Packer, "Photodamage to Microsomal Electron Transport Systems by Visible Light" (submitted to Photochemical Photobiology).

8. D. B. McCormick, "Interactions of Flavins with Amino Acid Residues: Assessments from Spectral and Photochemical Studies," Photochemical Photobiology, vol. 26, 1979, pp. 169-182.

9. E. G. Hrycay and P. J. O'Brien, "The Peroxidase Nature of Cytochrome P-420 Utilizing a Lipid Peroxide Substrate" Archives of Biochemistry and Biophysics, vol. 147, 1971, pp. 28-35.

10. R. J. Mehlhorn and L. Packer, "Photosensitized Nitroxide Spin Loss by Released Flavins in Mitochondrial Membranes" (in preparation).

11. R. J. Mehlhorn and L. Packer, "Membrane Surface Potential Measurements with Amphiphilic Spin Labels," Methods in Enzymology, vol. LVI, 1979, pp. 515-526.

12. T. H. Bothwell and C. A. Finch, eds., Chapter 9, Iron Metabolism, (Boston, Mass.: Little Brown and Co., 1962).

13. J. J. Maguire, E. W. Kellogg III, and L. Packer, "Evaluation of Pro-Oxidant Effects of Bound Iron" (in preparation).

LAKE ECOTOXICOLOGY RESEARCH

INTRODUCTION

J. Harte

The primary goal of the lake ecotoxicology projects is to develop and apply experimental methods for understanding and predicting effects of toxic substances on lake ecosystems. Both field and laboratory investigations comprise the research. Field studies focus mainly on mechanisms of acid precipitation damage in lakes on the western slopes of the California Sierra Nevada and the high Colorado Rockies. Laboratory work is focused on developing, validating, and applying innovative ecosystem-effects test systems. These test systems, involving laboratory ecosystems called "microcosms," are designed to allow more rapid, cheap, and statistically reliable prediction than field tests permit and to allow testing of more complex ecosystem-level effects than is possible with the single-species laboratory bioassays traditionally used.

The laboratory and field studies are tightly coupled in two ways. First, comparisons of the chemical and biological behavior of real lakes with microcosms allow us to assess the realism of microcosms, an essential step if these test systems are to provide an experimental basis for regulatory activity. Second, by adding simulated acid rain to lake microcosms, we are able to learn more about mechanisms of acid rain damage to natural lakes than could be learned from field investigations alone.

Theoretical modeling and policy analysis are a secondary, but not unimportant component of these projects. Mathematical models of the phenomena observed in the microcosms assist in the planning of experiments and in the extraction of useful damage indices from the raw data obtained from microcosm perturbation experiments. A nontraditional approach to statistical analysis of the often rapidly-time-varying biological parameters in microcosms and lakes has been developed by us and is now in use to provide measures of the realism and replicability of microcosms. Finally, policy implications of our work--particularly the freshwater constraints on energy development in the western United States--are addressed by us in publications and conference presentations.

ASSESSMENT OF OPTIMUM MICROCOSM DESIGN FOR POLLUTION IMPACT STUDIES*

J. Harte, D. Levy, J. Rees, and E. Saegebarth

INTRODUCTION

Laboratory microcosms may play an important role as experimental tools for examining ecological impacts resulting from human activities. The major advantage of microcosm studies over field research is that the former allow a greater opportunity for manipulation and control. In addition, the expense and environmental risk from microcosm investigations are relatively small compared to the risk from field studies of toxic substance effects. Microcosms also potentially offer greater realism than that provided by studies of impacts on single species.[1,2] Studies carried out with freshwater lake microcosms during a four-year period in our laboratory have been directed mainly toward developing and evaluating microcosms as toxicological testing systems.

Microcosms can be a useful tool for impact evaluation only to the extent that: (1) identically initiated systems replicate well, (2) the systems' biological and chemical behaviors, under both undisturbed and disturbed (with toxicant present) conditions, are similar to that of natural systems, (3) the attainment of (1) and (2) does not result in excessive complexity or cost. The degree to which the inherent drawbacks of microcosms reduce their usefulness, in the above sense, will depend on the manner in which microcosms are used. The specific objective of our research has been to investigate some of the major options for freshwater lake microcosm design and operation, emphasizing the ways in which the choices among these options influence the system's usefulness.

ACCOMPLISHMENTS DURING FY 1980

The major activity in FY 1980 was the completion of a two-year study of the realism and replicability of freshwater lake microcosms.[3] Only the upper pelagic zones (or water columns) of the lakes were modeled in these experiments--no sediments were included in the microcosms. Two local lakes (Briones and Lafayette Reservoirs)

*This work was supported by the Department of Energy under Contract W-7405-ENG-48 through the Energy Analysis and Environment Division of the Electric Power Research Institute under Contract No. RP 1224-1.

were used in this study. In three separate tests, replicate microcosms were initiated with water from these lakes, and the subsequent behavior of the lakes and microcosms was compared over three-month periods.

A number of different microcosm configurations were studied. The size of the microcosm containers (4 ℓ - 200 ℓ); the method of algal surface-growth prevention; and the degree of water mixing and aeration were the most important design and operating parameters explored. In addition, the microcosm-lake comparisons (or "tracking" studies) were carried out at various seasons, allowing us to determine the influence of natural seasonal factors, such as the washing of watershed nutrients into the lakes by winter rain, on the chemical and biological differences between the lakes and the microcosms.

Our most important findings were:

1. In microcosms greater than 15 l in volume, chemical and biological behavior is quite independent of microcosm volume if surface growth of algae on the inner walls of the microcosm containers is prevented by pouring the tank contents into a clean container at weekly intervals.

2. The amount of water agitation can influence the chemical and biological behavior of the microcosms; the optimum level of water mixing needs to be determined.

3. The week-by-week concentrations of chemical nutrients replicated well in all but the smallest microcosms and tracked (mimicked) the lake adequately except during periods when nutrient inputs to the lake from the surrounding watershed were high.

4. The patterns of phytoplankton succession in the microcosms adequately tracked those in the lake for up to 2 mo (a period adequate for many ecotoxicological tests) only when the physical conditions of the lake matched well those in the laboratory microcosm. Specifically, these lake conditions were: little runoff from the surrounding watershed, little water temperatures difference between lake and microcosms, and a well-defined, isolated epilimnion (upper part of the water column during the period when the lake water is thermally stratified).

During the late fall and winter in California, when the conditions listed in item 4 do not hold, diatom populations in the microcosms crashed within a month after initiation of the microcosms, while the diatom populations in the lake either bloomed or remained roughly constant. The lake behavior was probably due to replenishment in the upper water column of silica, an important limiting factor in diatom growth. Other factors that may have caused a discrepancy between the diatom populations in the lakes and in the microcosms were differences in water temperatures and zooplankton population densities. At the time of these experiments, our laboratory facility was incapable of bringing the microcosm water temperature down to winter-time levels. A new, improved microcosm cooling system now in operation permits matching in the laboratory of winter-time temperatures in the lakes. Figures 1 and 2 illustrate examples of excellent and poor tracking of lake diatom populations by the microcosms.

In order to compare the behavior of microcosms and lakes, appropriate statistical measures of "tracking" were needed. To illustrate the problem, consider a typical case in which three microcosms are set up in replicate using lake water. During the several months after initiation, weekly measurements of chemical and biological parameters in the lake and the microcosms are made. A suitable measure of tracking would involve a comparison between the replicate systems and the lake. One possible, and often used, procedure would be to average the microcosms over the three replicates and compare the average with the lake. Such a comparison could be made week-by-week or over time-averaged measurements. Because of measurements errors, and because of differences between

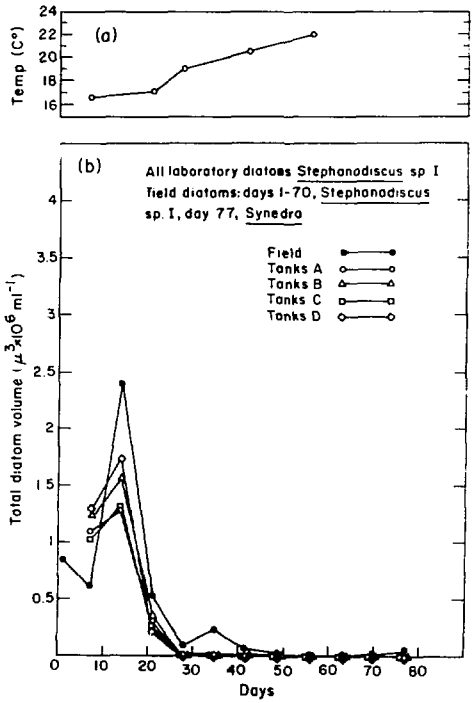

Fig. 1. Experiment 3. (a) Field temperature and (b) diatom populations for field and laboratory microcosms. Diatoms in both field and laboratory are all Stephanodiscus. Each point of the field data represents the mean of two samples. Each point of laboratory data represents the mean of three triplicate laboratory microcosms. (XBL 8012-2570)

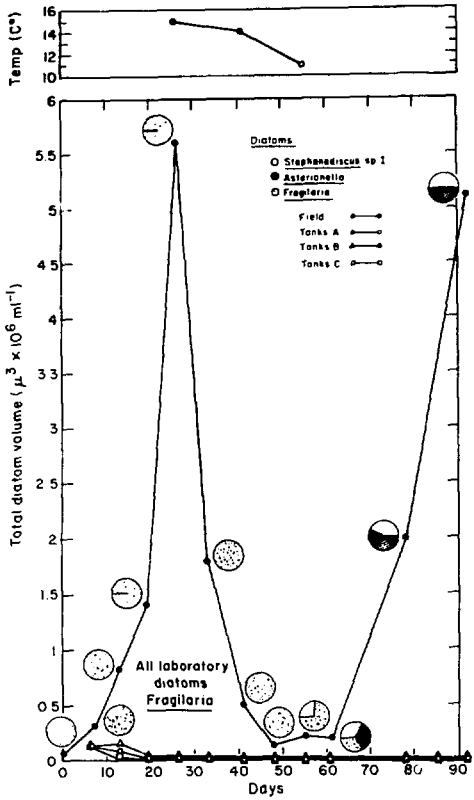

Fig. 2. (a) Field temperature and (b) diatom populations for field and laboratory microcosms. Each point of laboratory data represents the mean of three triplicate laboratory microcosms. All laboratory diatoms are Stephanodiscus. The circles above each field data point represent relative abundances of the designated diatom species. (XBL 8012-2573)

the replicate systems, there are standard deviations associated with each system's parameters. The difference between the lake and the averaged microcosms would have to be compared with microcosm and lake standard deviations in order to judge the statistical significance of the results.

In previous applications of this procedure, it had been assumed that each of the replicate microcosms are in fact the same system, with the same true mean values of each parameter. Differences among them are ascribed, in effect, to measurement error only. If that assumption is not made, and instead each of the three replicate system's true mean is taken to be its measured mean, then statistical significance tests can give quite different results. This is particularly true if, as is the case with most of our chemical and biological measurements, the measurement errors are strongly dependent on the mean values of the parameters. The result of our assumption is that the significance test for tracking is more stringent. That is, a situation that would have been deemed good tracking with the previous assumption might be considered poor tracking with ours. The previous procedure has been in widespread use, in many contexts in biology, because it is simpler to carry out. Nevertheless, our revised procedure is more appropriate to the conditions of the experiments.[4]

Our experimental results over the past two years have demonstrated that lake microcosms are inappropriate for certain types of toxicological testing. In particular, long-term tests, extending beyond several months, cannot be carried out because lake microcosms do not function similarly to natural lakes for such extended periods. Moreover, experiments involving macrofauna, such as fish, cannot be carried out in laboratory-sized systems (up to 1000 liters) without distorting the behavior of the system by the presence of the macrofauna. A type of test that is particularly appropriate to microcosms is a determination of the effects of a toxic substance on the rate of decomposition of organic matter and the related production rate of inorganic nutrients. Such nutrient cycling processes in lakes generally take place by the microorganisms' action on detritus. Because of the great importance of these processes to ecosystems' overall health and productivity; because the microorganisms and their chemical environment can be represented realistically in microcosms; and because nutrient regeneration processes take place relatively rapidly on the time scale of lake dynamics, we have begun exploring a possible microcosm test protocol for determining effects of toxicants on nutrient recyling rates in lakes.

Work carried out in FY 1979 demonstrated that additions of lake detritus to lake microcosms, followed by measurements of the nitrogen budget on a daily basis for a week or two provided considerable information about the population biology of the microorganisms responsible for the decomposition and nutrient regeneration activity.[5] This year, attention was focused on constructing a mathematical model of the microorganism-detritus-nutrient system to yield results consistent with the wealth of experimental information available from the detritus-addition studies. The goal of this modeling effort is to learn how to extract from the detritus-addition experiments useful indicea characterizing the health of the nutrient cycling function in the system. This will allow development of a test procedure, involving simultaneous additions to lake microcosms of detritus and toxic substances, for determining the damage to the nutrient cycling function caused by the toxicant.

The results to date have been encouraging. A relatively simple mathematical model has been constructed that is capable of fitting the complex behavior seen in the experiments.[6] Moreover, a wide class of models based on assumptions that are plausible but different than ones reflected in the successful model, have been shown to be inadequate. With this model, we are now able to extract from the experimental results the needed damage indices.

Two experimental advances in lake decomposition research took place in FY 1980. In order to perform the detritus-addition experiments, large amounts of concentrated dissolved lake-water organic matter need to be obtained. Off-the-shelf organic chemicals are inadequate for the purpose as they lack the biochemical diversity characteristic of real lake detritus. After pursuing a number of dead ends, we found a suitable approach based on successive freeze concentrations of lake water.[7]

The second advance was a method of "fingerprinting" lake organic matter. Adapting an approach developed by the Atmospheric Aerosol Research group, we took a number of carbon and nitrogen thermographs of water samples from local lakes and from pure algal cultures. Information obtained from thermography is intermediate in complexity between simple total C and N analysis and a complete gas chromatography analysis of organic constituents. Our preliminary studies (using only about a dozen tests to date) suggest that thermography may provide a characteristic fingerprint that differs from one type of alga to another and that varies with the amount of decomposition of an algal sample. A more intensive effort to develop this technique for ecological materials is warranted.

In FY 1980, heightened national concern over effects of toxic substances in the environment led the National Academy of Sciences to convene an 11-member Panel on Ecotoxicology; J. Harte was appointed as one of the members. Its task was to make recommendations to the Environmental Protection Agency (EPA) on how best to implement the ecologically relevant sections of the Federal Toxic Substance Control Act. A major part of the year-long effort was devoted to evaluating the role of microcosms as test systems for toxicant pathways, fate, and effects studies. The panel's final report is in preparation.[8] Three reports written by members of the LBL lake ecotoxicology group will also appear as appendices to the report.[9,10,11] In conjunction with this National Academy effort, Oak Ridge National Laboratory (ORNL) conducted a review of prior work in the area of microcosms; D. Levy assisted in that review process.

Expected Progress in FY 1981

The major focus of research in FY 1981 will be on extensions of aquatic microcosms to include lake sediments. Our lake microcosms to date have been models of the pelagic zone, or water column, of lakes. Because of the importance of lake sediments as a source of nutrients to the pelagic zone at certain times of year, as a sink of pollutants, and as a site in which pollutants can be transformed or can enter the aquatic food chain via benthic organisms, it is vital to have the capability of modeling the sediment zone as well as the overlying water. Doing so is not a trivial task. Microcosms are considerably shallower than real lakes, and therefore if sediments are simply placed along the bottom of a microcosm they will exert an exaggerated influence on the overlying water. The approach we will follow is similar to one that has been shown to work for marine estuarine microcosms at EPA's Naragansett Bay laboratory in Rhode Island.[12] The basic idea is to place the sediments in small chambers, with portals carefully adjusted to provide a level of flushing that will allow oxygen levels in the microcosm sediments to match those in the lake sediments.

During FY 1981, experimental studies of benthic lake microcosms will begin. Two types of microcosms will be studied. In one, water and sediments from a shallow cove in Briones Reservoir will be placed in microcosms. In the second, a deep-water site will be chosen and sediments plus water from the hypolimnion (the stratified layer of lake water overlying the sediment) will be placed in microcosms. The replicability of these systems and the degree to which they can be designed and operated to track the lake will be investigated.

Of particular interest in these studies will be the degree to which the chemical composition of the water within and immediately overlying the sediments is the same in the microcosms and the lake. If benthic microcosms are to be of use in ecotoxicology, it is essential that oxygen levels in the chemically active benthic zone match well those in natural systems. For this reason, we will design benthic chambers to house the sediments in such a manner as to allow adjustments of the oxygen levels. This will be accomplished by means of the portals mentioned. A related variable to be adjusted so as to maximize the microcosms' realism is the degree of water-mixing in the microcosms. Our past work has shown that this variable can influence biological behavior in the microcosms;[3] in FY 1981, research to determine an optimum level of water mixing will commence. Optimality will again be determined by the twin criteria of realism and replicability.

Among the variables of interest in these planned benthic studies is the diatom population. Because sediments are a source of silica, we hypothesize that the diatom populations will behave more realistically in the benthic systems than in our pelagic microcosms tested previously.

In these tracking studies, Briones Reservoir will again be the source of microcosm water and the system against which microcosms will be compared to assess their realism. Research to characterize the chemical and biological parameters of Briones will continue in FY 1981. The major focus will be to determine the degree of spatial (horizontal and vertical) and temporal (diurnal and seasonal) variation in chemical concentrations and species composition. This information is needed in order to design a lake-monitoring schedule that will minimize expended effort and yet will be sufficiently thorough so as to provide an accurate characterization of the significant ecological processes in the lake. Moreover, this information will assist in selecting the best method for initiating the microcosms--for example, choosing between stocking the microcosms with a depth-integrated sample from a particular stratified layer or working with water from only one depth.

In FY 1981, further study of detrital thermographs will be undertaken. The major effort here will be to determine the degree to which different lakes, and the same lake at different times of the year, yield characteristically different thermographs of their dissolved and suspended detrital matter. In related work, using our freeze-concentration method for preparing detritus, additional decomposition experiments will be carried out. Our recently-developed mathematical model, while consistent with the previously-measured phenomena, makes several detailed predictions, which we will test in FY 1981.

REFERENCES

1. M. Dudzik, J. Harte, A. Jassby, E. Lapan, D. Levy, and J. Rees, "Some Considerations in the Design and Aquatic Microcosms for Plankton Studies." International Journal of Environmental Studies, vol. 13, 1979, pp. 125-130.

2. J. Harte, D. Levy, J. Rees, and E. Saegebarth, "Making Microcosms an Effective Assessment Tool," Microcosms in Ecological Research, J. P. Giesy, ed. (in Press).

3. J. Harte, D. Levy, J. Rees, and E. Saegebarth, "Assessment of Optimum Aquatic Microcosms Design for Pollution Impact Studies," a report to the Electric Power Research Institute (Palo Alto, Calif: Electric Power Research Institute, 1980).

4. D. Levy, "Appropriate Statistical Methods for Ecological Microcosm Investigations" (in preparation).

5. J. Harte and D. Levy, "Investigation of the Responses of Lake Waters to Detritus Additions," Energy and Environment Division, Lawrence Berkeley Laboratory, Berkeley, Calif., 1979 (to be submitted for publication).

6. J. Harte, "Modeling the Response of Lake Water to Organic-Matter Loading" (in preparation).

7. R. Schneider, "A Method for Concentrating Freshwater Lake Detritus for Microcosm Research," Energy and Resources Group Research Report, University of California, Berkeley (in preparation).

8. J. Cairns, M. Alexander, K. Cummins, W. T. Edmondson, C. Goldman, J. Harte, R. Hartung, A. Isensee, R. Levins, J. F. McCormick, T. Peterle, J. Zar, Testing Effects of Chemicals on Ecosystems. A Report by the Committee to Review Methods in Ecotoxicology, National Academy of Sciences - National Research Council, Commission on Natural Resources, Washington, D. C., 1980.

9. P. Gleick, "Lakes and Microcosms: Extending Microcosm Data to Aquatic Ecosystems," (to appear as an appendix to reference 8).

10. R. Schneider, "Classes of Ecotoxicological Tests: Their Advantages and Disadvantages for Regulation," (to appear as an appendix to reference 8).

11. J. Harte, "Optimum Microcosms for Lake Ecotoxicology," (to appear as an appendix to reference 8).

12. K. T. Perez et al., "The Importance of Physical and Biotic Scaling in Experimental Simulation of a Coastal Marine Ecosystem." Helgolander wiss Meeresuuters, 30, 1977, pp. 144-162.

ACID PRECIPITATION DAMAGE TO AQUATIC ECOSYSTEMS*

J. Harte, K. Tonnessen, R. Schneider, G. Lockett, and J. Oldfather

INTRODUCTION

Present evidence suggests that high-elevation aquatic ecosystems are particularly vulnerable to human disruption. In the Eastern United States, acidic rain and snowmelt have lowered the pH of water bodies at the higher elevations in the Adirondack Mountains. This has resulted in loss of certain species of fish,[1] leaching of metals from soils, suspension of metals from sediments,[2] and altered rates of decomposition activity.[3]

Research on artificially acidified water bodies (streams and microcosms) indicates significant export of nutrients and biomass from acidified regions[4] and mobilization of metals from sediments.[5,6] Alterations of plankton populations have also been observed under acidic conditions. In addition to acid precipitation, trace metals and hydrocarbons released during coal combustion can affect aquatic systems, including the possibility of their biomagnification within aquatic foodchains.[7] Despite the accumulating evidence for acid precipitation damage to certain aquatic ecosystems, present understanding of the mechanisms of transport and effect are far from adequate.

Two research efforts to study acid precipitation effects in high-elevation aquatic ecosystems

*This work was supported by the Department of Energy under Contract No. W-7405-ENG-48 through the California Policy Seminar.

are underway at Lawrence Berkeley Laboratory (LBL). One goal of this research is to establish baseline conditions against which changes can be detected should they occur. A second and related goal is to develop from the pattern of such changes and from associated laboratory studies an increased understanding of the mechanisms and progression of acidification and its impacts on high-elevation aquatic ecosystems.

ACCOMPLISHMENTS IN FY 1980

Acid Precipitation Effects in the Sierra Nevada

Field and laboratory research on the potential for acid-precipitation damage to aquatic systems of the Sierra Nevada, California was carried out by K. Tonnessen and J. Oldfather. Twenty lakes on the Sierra's western slope were characterized during the 1980 field season with reference to pH, temperature, alkalinity, trace metal concentrations, phytoplankton populations and sediment composition. None of the lakes sampled had a pH less than 6.0, although alkalinities were low. Some of the lakes sampled were found to have high iron levels in the water column.

These field analyses formed the basis for selecting Mosquito Lake (8500 ft) as one of the three lakes to be modeled in the laboratory using microcosm systems.

Twelve 18-l systems using water taken from Mosquito Lake were established in a room with controlled light (10 h light: 14 h dark) and controlled temperature (8° C). Six replicate tanks (three with sediment, three without sediment) were treated with sufficient HNO_3 to reduce the system pH to 4. Six control tanks, with and without sediment, were left untreated. During a 6-week period, changes in pH, metals, and phytoplankton and zooplankton species were monitored weekly.

Analysis of data from previous microcosm experiments was completed and the results presented at a national meeting of the American Water Resources Association in Minneapolis, Minn. in October 1980[6] and at the International Symposium on the Ecological Effects of Acid Precipitation, Sandefjord, Norway, March 1980.[8]

Acid Precipitation Research on Colorado Alpine Aquatic Ecosystems

Three researchers from the LBL aquatic ecology group designed and initiated a research program to investigate acid precipitation impacts on Colorado alpine aquatic ecosystems. The scope of the research is to monitor a number of meteorological, chemical, and biological variables that characterize a selected alpine watershed over a period of up to twenty years. The site selected is the Mexican Cut/Galena Mountain Research Preserve, a hydrologically self-contained watershed spanning the elevations from 3200 to 3800 m (approx.) on the Rocky Mountains' western slope. The watershed contains a lake of about 30,000 m^2 situated above timberline; a series of ponds below timberline in a subalpine forest of Englemann spruce and alpine fir; and a drainage creek (see Fig. 1). The Preserve is located approximately 25 km southwest of Aspen, Colo. and 15 km north of Crested Butte, Colo.

Measurements made during the summer of 1980 showed rain pH to be 4.0 - 4.6 with 4.2 the most common value. Snow core pH measurements were 5.6 - 5.9. However, these measurements were taken in mid-June after considerable snow melting had occurred, and good evidence exists that the majority of the ions are released during the early part of the melt.[3] It would appear from our measurements, therefore, that acid stresses are occurring on the western slope of the Rockies. Data of other investigators on the eastern slope of the Rockies show similar results.[10]

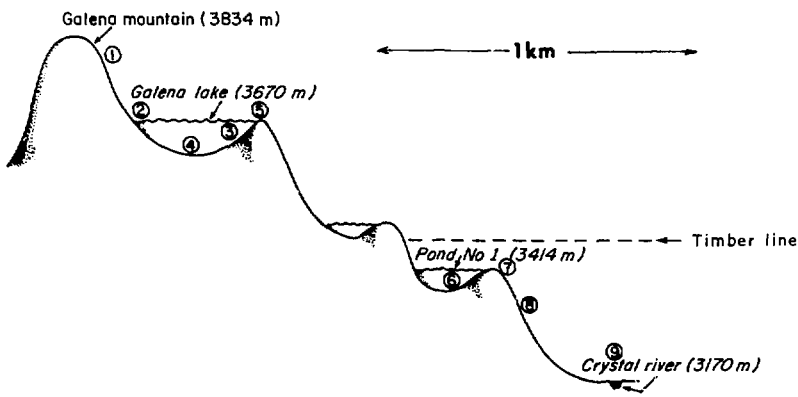

Fig. 1. Cross section of the Galena/Mexican Cut watershed showing research sites. (XBL 8012-2567)

pH measurements in the surface waters gave values ranging from 5.6 at the higher elevations (snow-melt) to more than 7 at the lower elevations (see Fig. 2). During 1980 we began to characterize the buffering capacity of the watershed. As measured by alkalinity, the buffering capacity ranged from a low of <30 microequivalents/l in Galena Lake to over 200 in the ponds (see Fig. 3). The low values above timberline indicate that those water bodies are especially vulnerable to acid loading. The higher values at the lower elevations are caused by more extensive soil development in the forest and by increasing organic content of the water. The bedrock is primarily metamorphosed quartzite, siltstone, and shale; these minerals are quite resistant to weathering and provide little buffering capacity.

Water and snow samples from various sites were collected for metals analyses, which are now underway. These measurements are a regular part of the monitoring effort to determine if there exist significant airborne metals deposition, soil leaching, and/or sediment mobilization.

Populations of salamanders have proven to be useful indicators of acid precipitation damage in aquatic systems of the northeast U.S.[11] Large populations of Ambystoma tigrinum (tiger salamander) inhabit a number of the ponds in the Preserve. During the summer of 1980, a salamander census in Pond #1 conducted three times at about weekly intervals yielded a population of 230 ± 20 individuals.

In summary, during 1980 a research program into acid precipitation impacts was designed; analytical methods were selected and tested; field and base laboratories were established; sampling strategies were chosen, and preliminary data were collected.

PLANNED ACTIVITIES FOR FY 1981

Acid Precipitation Effects in the Sierra Nevada

Acid-precipitation effects research will continue in both the laboratory and the field. Two additional Sierra lake microcosm experiments will

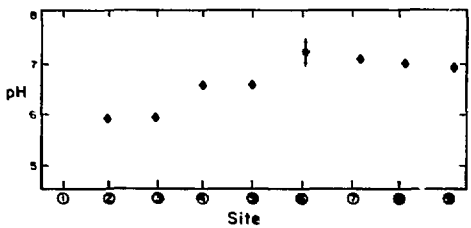

Fig. 2. Results of pH measurements at the nine sites (see Fig. 2) during the summer of 1980. The ♦'s represent averages over weekly measurements, but except for site-6, the variation from week to week was insignificant.
(XBL 8012-2565)

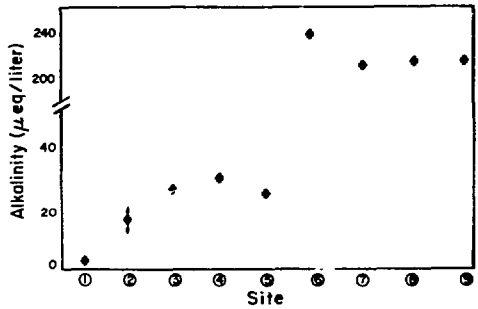

Fig. 3. Results of alkalinity measurements at the nine sites (see Figure 2) during the summer of 1980. The ♦'s represent averages over weekly measurements, but except for site 2, the variation from week to week was insignificant.
(XBL 8012-2564)

be carried out in 18-l systems, with and without sediments. Sediment composition, determined by neutron activation analysis, will be an important consideration in the selection of sensitive western slope lakes. Metals resuspension from lake sediments will be monitored following system acidification. The impact of pH and metals concentration changes on the biological populations will be monitored.

Additional western slope lakes will be sampled in 1981, with emphasis being placed on sampling during the spring melt period. In other regions of North America and in Scandinavia, the low pH of runoff water during this period has proven to be a crucial factor in lake acidification process. Sampling in the western Sierra will indicate whether a similar situation exists in the western U.S.

A cooperative effort in acid precipitation field research in the Sierra will be established with Dr. John Melack of the University of California at Santa Barbara. The extent of the acid precipitation problem in California will be explored at the California Symposium on Acid Precipitation to be held January 14-15, 1981. A report on the activities of the LBL Group will be presented at this symposium.

Acid Precipitation Research on Colorado Alpine Aquatic Ecosystems

Meteorological sampling stations will be set up to measure precipitation volumes and to collect samples for ion and metals analysis. Snowpack and spring snowmelt will be similarly analyzed. Regular monitoring of pH, alkalinity, and metals concentration in surface waters will occur. Further characterization of the buffering capacities and metals content of watershed soils and of lake and stream sediments will be made. Attempts will be made to understand the relative contributions of mineral, organic, and carbonic acids to the total buffering capacity of the water bodies.

Nutrient export rates in the forms of inorganic nitrogen (NO_3 + NO_2, NH_3) and total phosphorous concentrations will be measured in the drainage creek. These measurements will indicate whether significant downstream export of nutrients from the watershed is occurring, a phenomenon observed in artificially acidified water bodies.[4] A series of microcosm experiments will be performed to determine changes in the mineralization potential of the Galena water column. Standard additions of organic substrates will be made to lakewater aliquots, and the evolution of inorganic nutrients will be measured. If evolution of inorganic nutrients decreases with time, this will be an indication that lake decomposition processes are being affected, as reported elsewhere.[3]

Population counts of salamanders in Pond #1 will be made on a biweekly basis. Monitoring of lake and pond phytoplankton and zooplankton and of stream insects will be done by other members of our research team. Further refinements of field methods will be undertaken.

A Model of Watershed Acidification

A watershed subjected to continuing acid precipitation will neutralize the acids as long as sufficient alkalinity, or buffering capacity, is present in the lake and stream waters, the watershed soils, and the lake sediments. As the buffering capacity is gradually overwhelmed by acids flowing through the system, a threshold is reached at which a sudden, large drop in the pH of the water bodies takes place. Developing the ability to predict the time to reach threshold is an important task in acid precipitation research. The approach of the system to the threshold is not well understood. Even at relatively well-studied sites, experimental information is incomplete regarding some of the critical steps in the buffering process (such as the rate of deposition of atmospheric alkaline materials, or the influence of lake sediments on the buffering of the overlying water column). However, even with an adequate data base, predicting the time to reach threshold would not be simple because of the diversity of both competing and reinforcing processes. Needed is a reliable mathematical model capable of describing the linkages among these processes. The development of such a model, incorporating only empirically accessible rate parameters and variables, will be carried out in FY 1981. During the summer of 1981, baseline values for the model components will be measured at the Galena/Mexican Cut watershed; in subsequent years, model predictions will be confronted with experimental measurement.

REFERENCES

1. C. L. Schofield, "Lake Acidification in the Adirondack Mountains of New York: Causes and Consequences," in L. S. Dochinger and T. A. Seliga, eds. Proceedings of the First International Symposium on Acid Precipitation and the Forest Ecosystem, United States Department of Agriculture Forest Service Technical Report NI-23, 1976.

2. C. S. Cronan and C. L. Schofield, "Aluminum Leaching Response to Acid Precipitation Effects on High Elevation Watersheds in the Northeast," Science, vol. 204, pp. 304-306.

3. F. H. Braekke, Impact of Acid Precipitation on Forest and Freshwater Ecosystems in Norway, Research Report 6, 1432 AAS-NLH, SNSF Project, Norway, 1976, (Available from SNSF Project, Box 61, 1432 As-NLH, Norway.)

4. R. J. Hall, and G. E. Likens, "Chemical Export in an Acid-Stressed Stream" (submitted to Science, 1980).

5. A. O. Davis, J. N. Galloway, and D. K. Nordstrom. "Lake Acidification: Its Effect on Lead Mobility in the Sediment of Two Adirondack Lakes," Limnology and Oceanography (in press), 1980.

6. K. Tonnessen and J. Harte, "The Potential for Acid Precipitation Damage to Aquatic Ecosystems of the Sierra Nevada, California," abstract of paper presented at Annual Meeting of the American Water Resources Association, October 12-16, 1980.

7. Office of Technology Assessment (OTA), The Direct Use of Coal, prepared for U.S. House of Representatives Committee on Science and Technology, U.S. Government Printing Office, Washington, D.C., 1979.

8. K. Tonnessen and J. Harte, "The Potential for Acid Precipitation Damage to Aquatic Ecosystems of the Sierra Nevada, California (USA)," Proceedings of the International Conference on the Ecological Impact of Acid Precipitation, Sandefjord, Norway, March 11-14, 1980 (in press), (December 1980).

9. W. M. Lewis, Jr., and M. C. Grant, "Changes in the Output of Ions from a Watershed as a Result of the Acidification of Precipitation," Ecology, vol. 60, no. 6, 1979, pp. 1093-1097.

10. F. H. Pough, "Acid Precipitation and Embryonic Mortality of Spotted Salamanders, Ambystoma Maculatum," Science, vol. 192, pp. 68-70.